

# Towards an improved ASCAT wind product under rain conditions

Marcos Portabella (ICM-CSIC)

Wenming Lin (ICM-CSIC)

Ad Stoffelen (KNMI)

Antonio Turiel (ICM-CSIC)

Anton Verhoef (KNMI)

David Weissman (Hofstra University)

# Rain impact on ASCAT derived-winds (for low and moderate rain rates)

- Increased wind variability
- Sea surface rain “splashing”

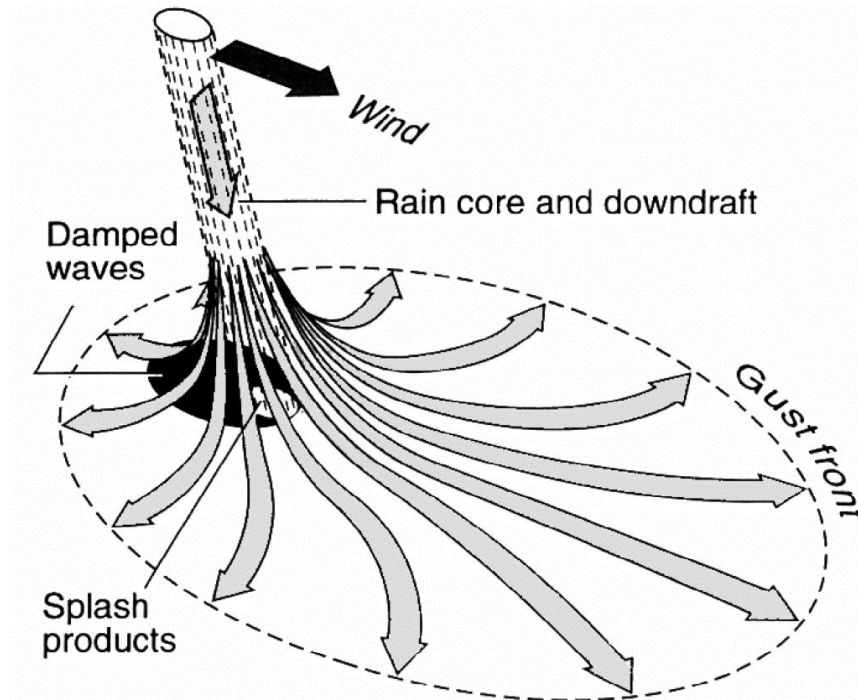
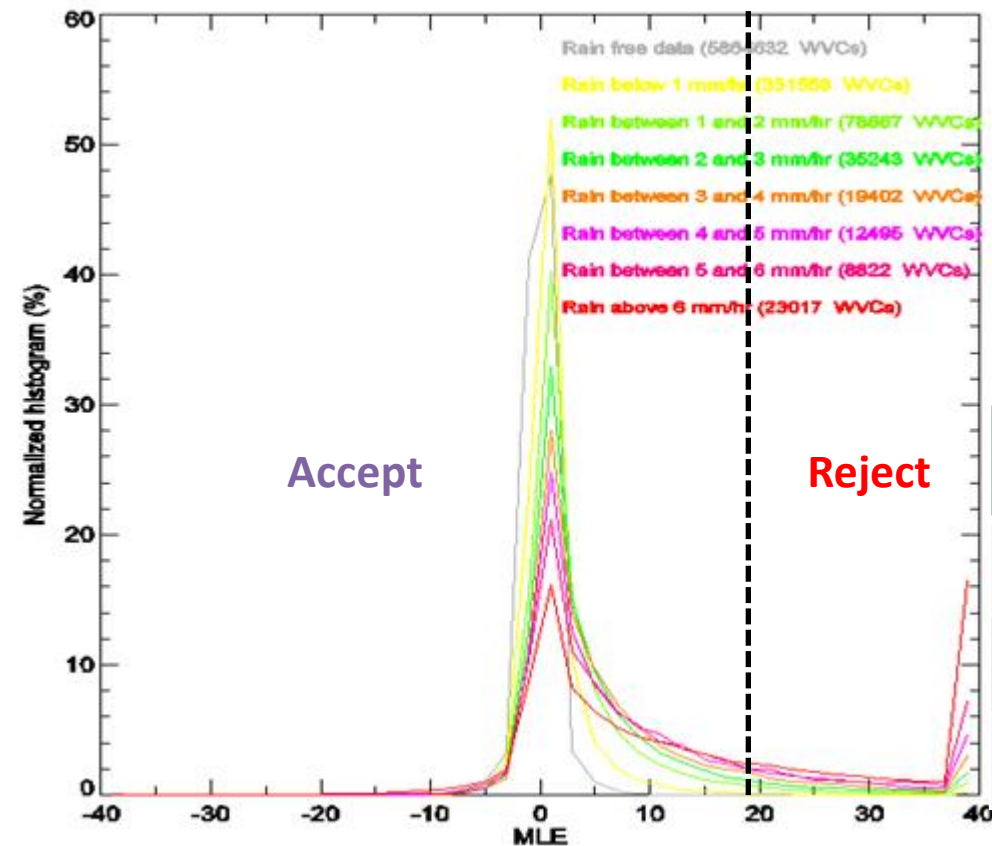
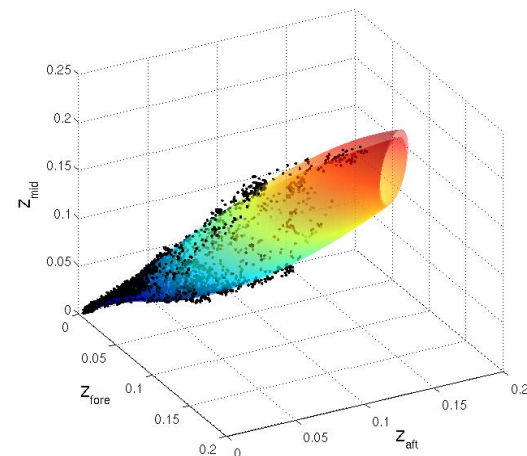


Figure 17.1. Schematic sketch of the downdraft associated with a rain cell. The downdraft spreads over the sea surface, causing an enhanced roughening of the sea surface and, thus, an increase in the backscattered radar power [After *Atlas*, 1994b].

# Why complementary method to MLE-based QC method?



Validation: ASCAT-TMI



Category	Accept		Reject	
	Number	VRMS	Number	VRMS
Rain-free	2442	1.81	0(0)	/
Vicinity of rain	413	2.67	1(1)	/
Rain	181	4.36	11(10)	6.63

Validation: ASCAT-Buoy

# Singularity analysis

- Concept

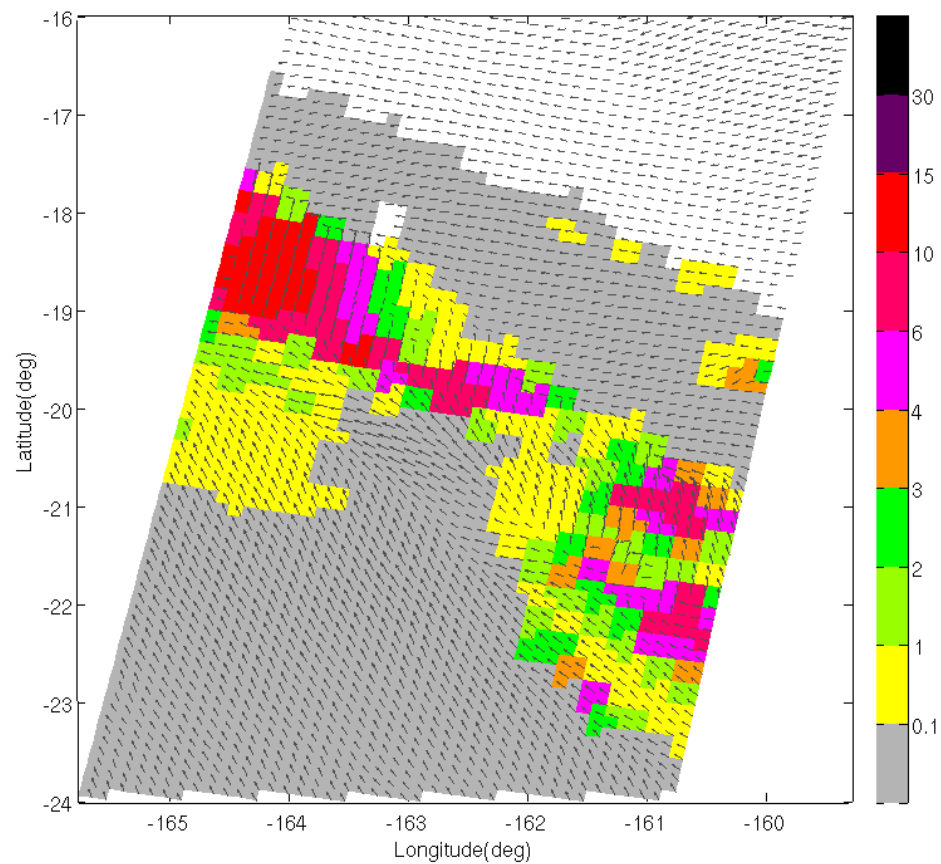
Given a wavelet  $\Psi(\mathbf{x})$ , we define the wavelet projection of the gradient of a two-dimensional scalar signal  $s$  at the point  $\mathbf{x}$ , and the scalar  $r$ , as

$$T_{\Psi}|\nabla s|(\mathbf{x}, r) = \int d\mathbf{y} |\nabla s|(\mathbf{y}) \frac{1}{r^2} \Psi\left(\frac{\mathbf{x} - \mathbf{y}}{r}\right)$$

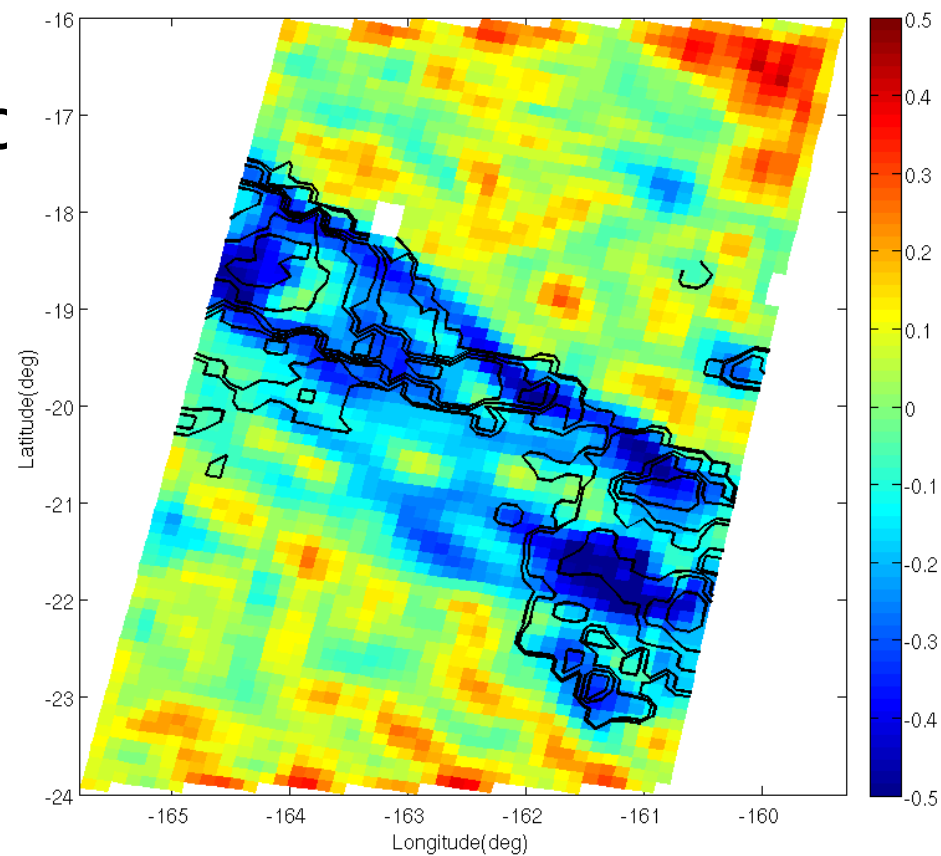
where the wavelet projection depends on the scale resolution parameters as a power law, characterized by the local singularity exponent  $h(\mathbf{x})$  in the way

$$T_{\Psi}|\nabla s|(\mathbf{x}, r) = \alpha(\mathbf{x}) r^{h(\mathbf{x})} + o(r^{h(\mathbf{x})})$$



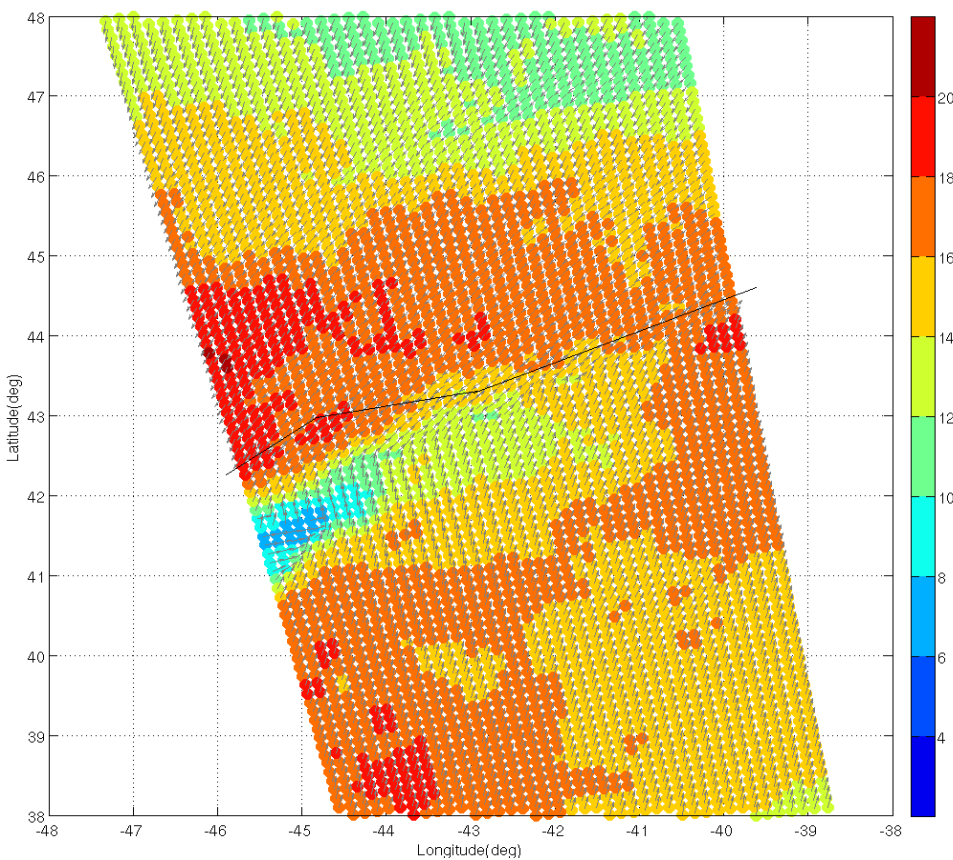


ASCAT-derived wind field collocated  
with TMI RR data at 20:30 UTC on 24  
September 2008

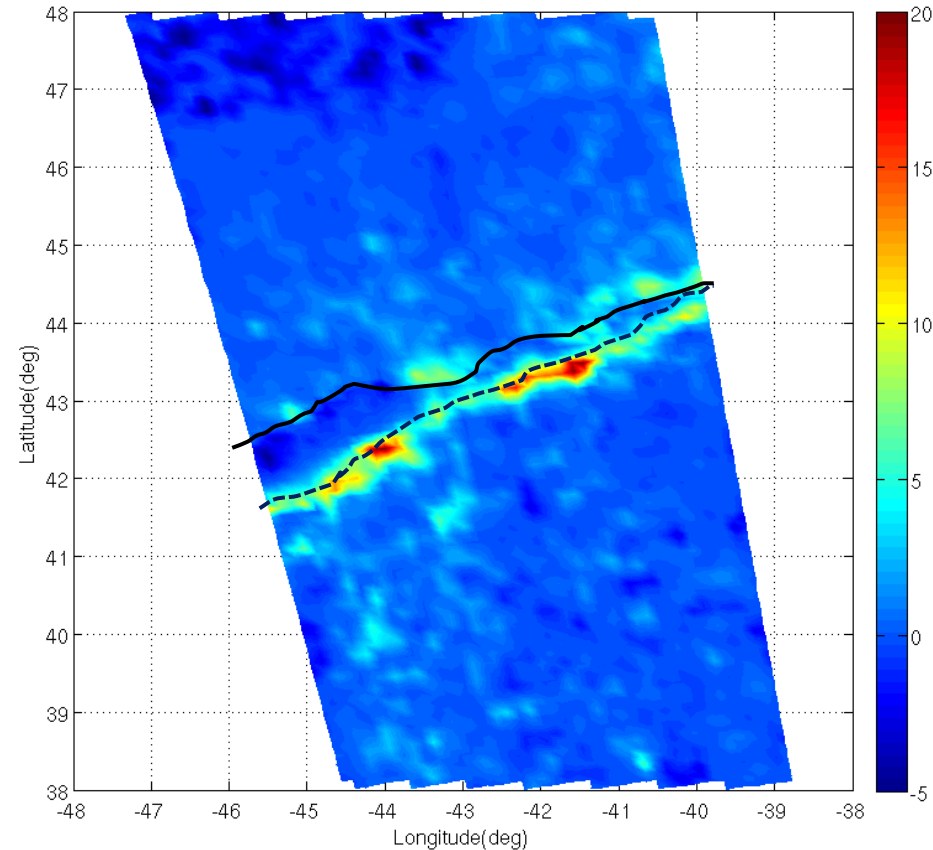


Singularity map of the ASCAT-retrieved  
wind field. TMI RR data shown as contour  
lines

- **Good correspondance between TMI RR and negative SE values**

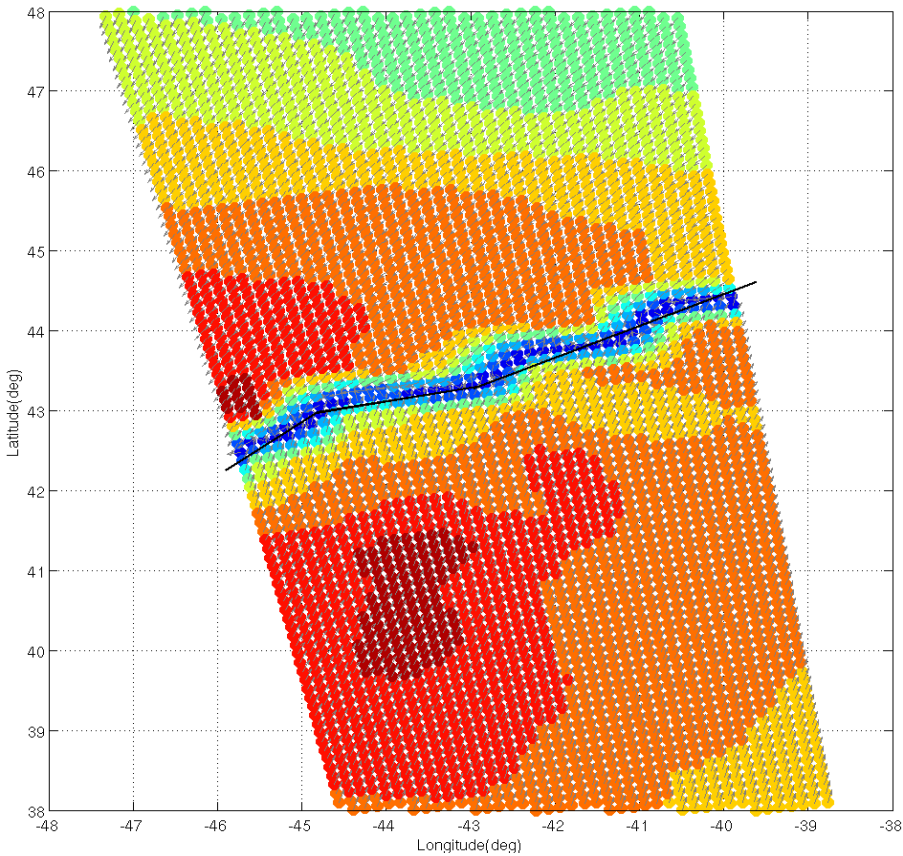


ASCAT-derived wind field at 00:15  
December 15 2011

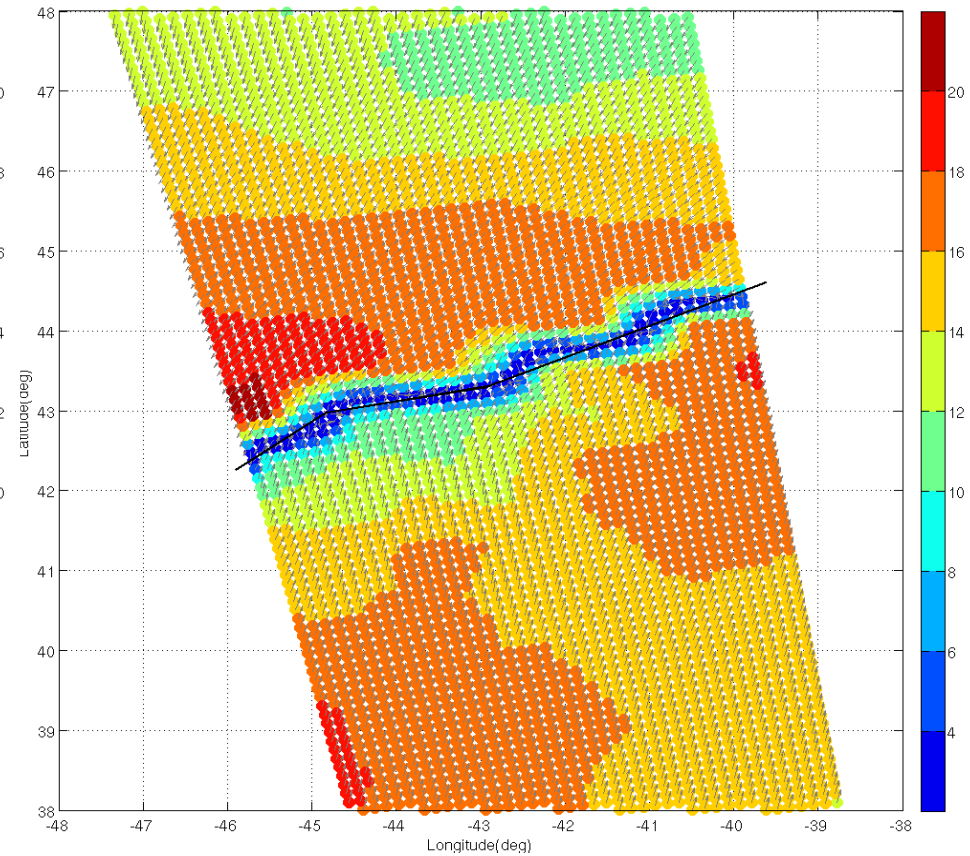


ASCAT-derived MLE distribution

- Solid line shows ASCAT-derived wind front (convergence)
- Dotted line shows front as detected by MLE analysis



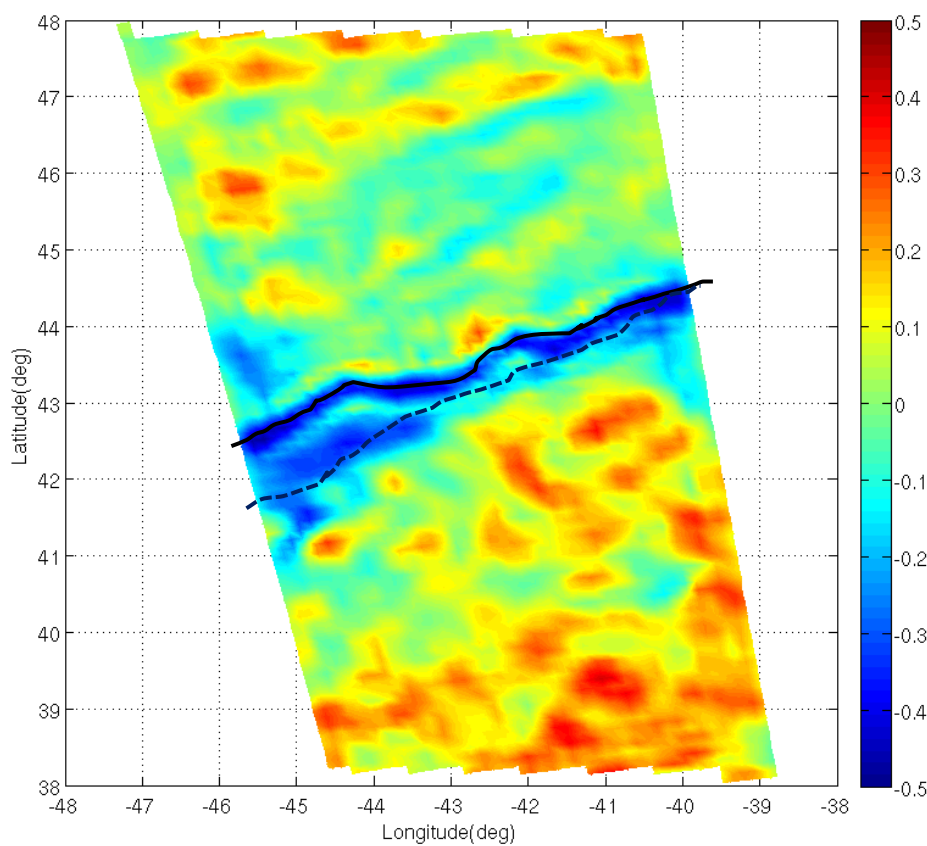
Collocated ECMWF wind field



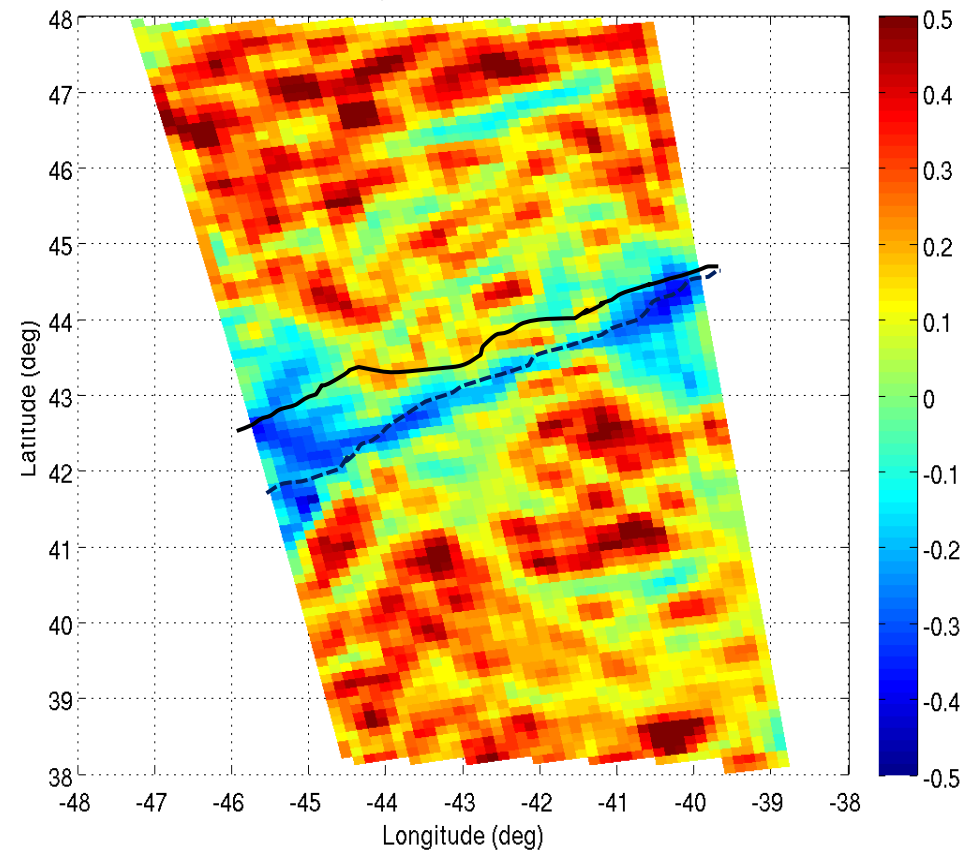
ASCAT 2D-Var analyzed wind field

- ECMWF front misplaced
- ASCAT 2D-Var field shows front in same position as ECMWF
- Ambiguity removal error -> ASCAT front misplaced

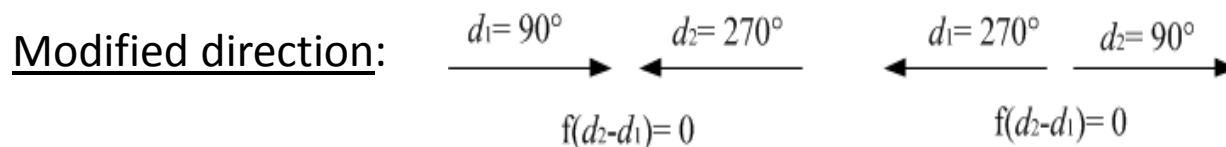




Singularity map from ASCAT U and V

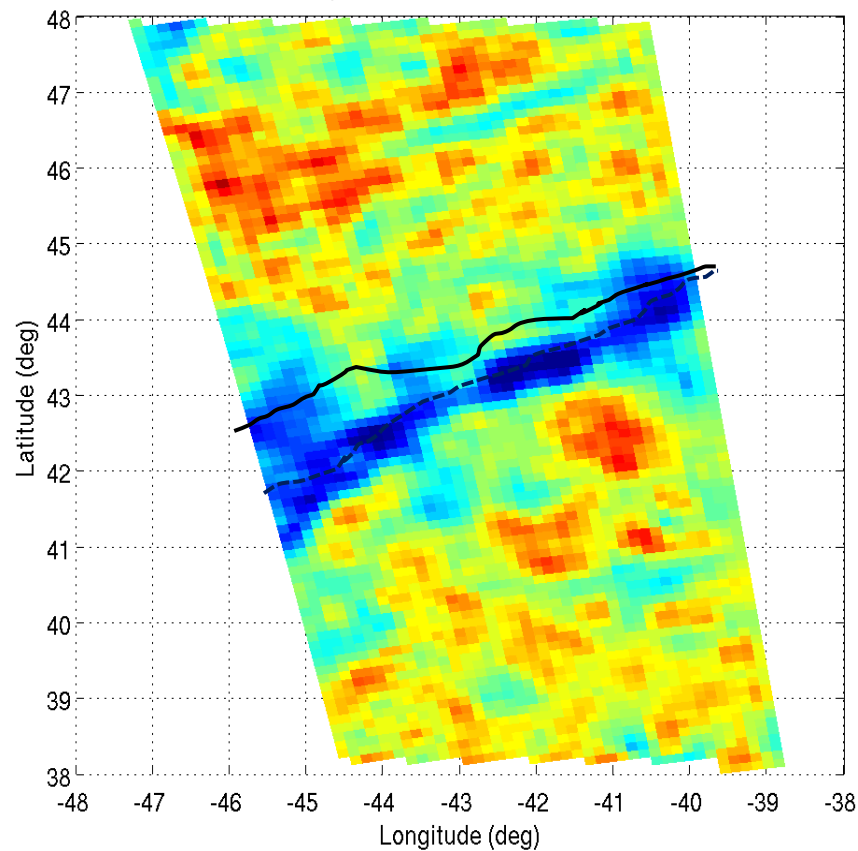


Singularity map from modified  
ASCAT direction

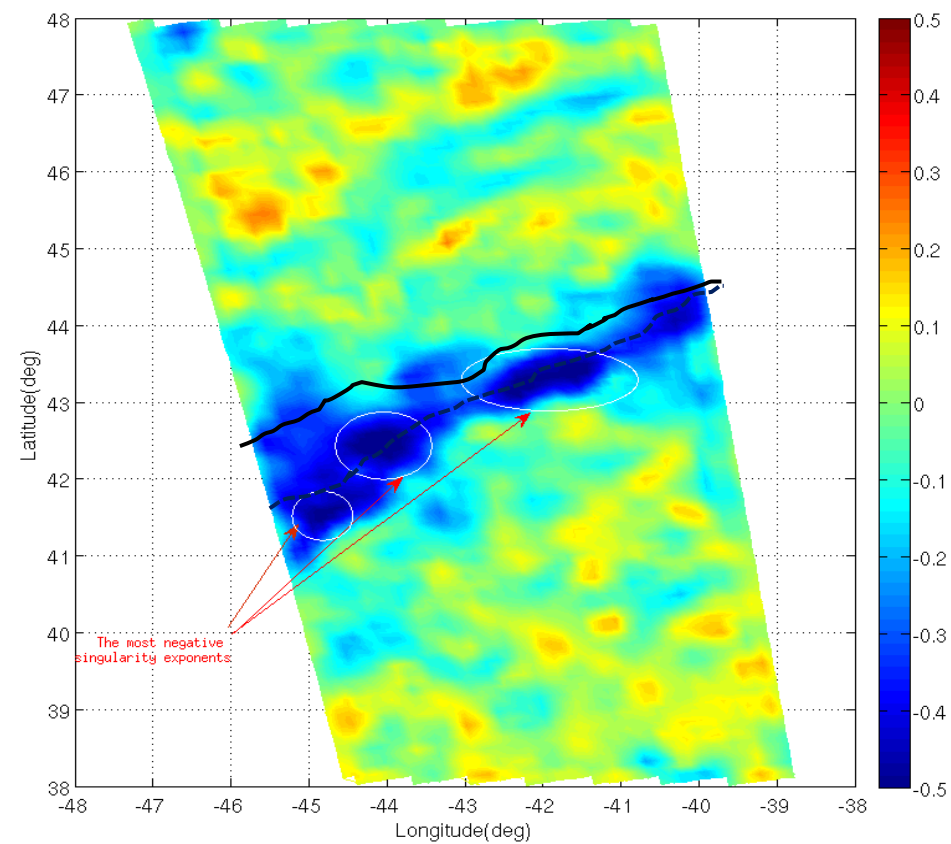


- AR errors propagate into singularity analysis computation
- Modified direction insensitive to AR errors



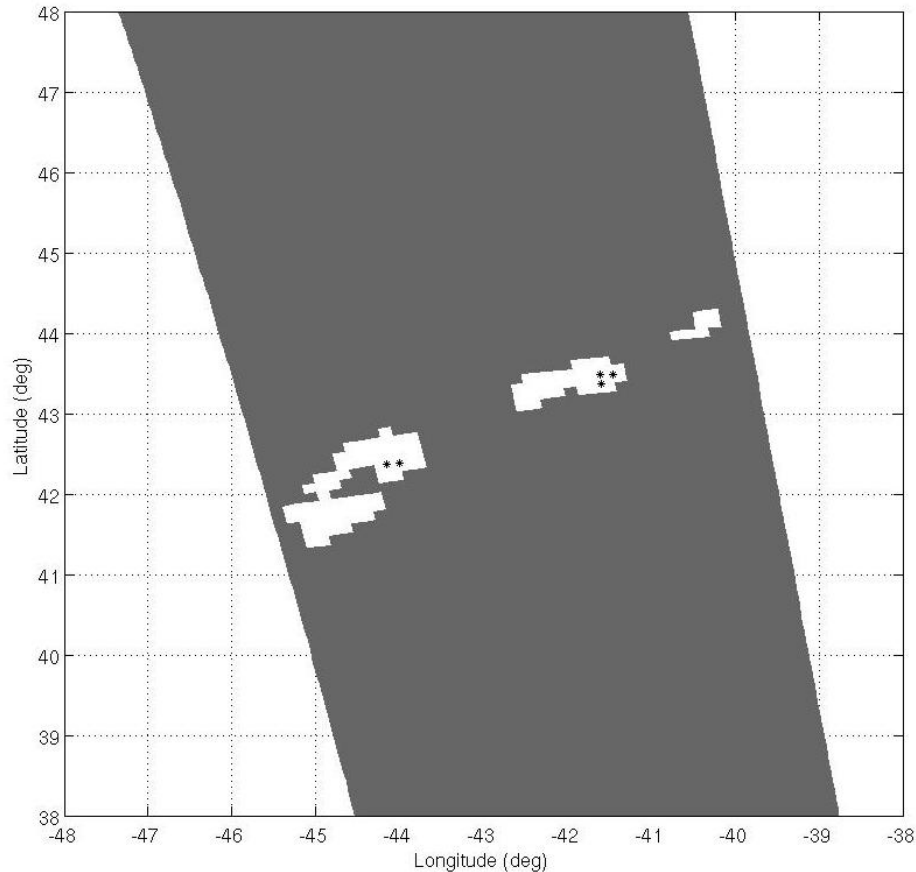


Singularity map from modified wind direction and MLE

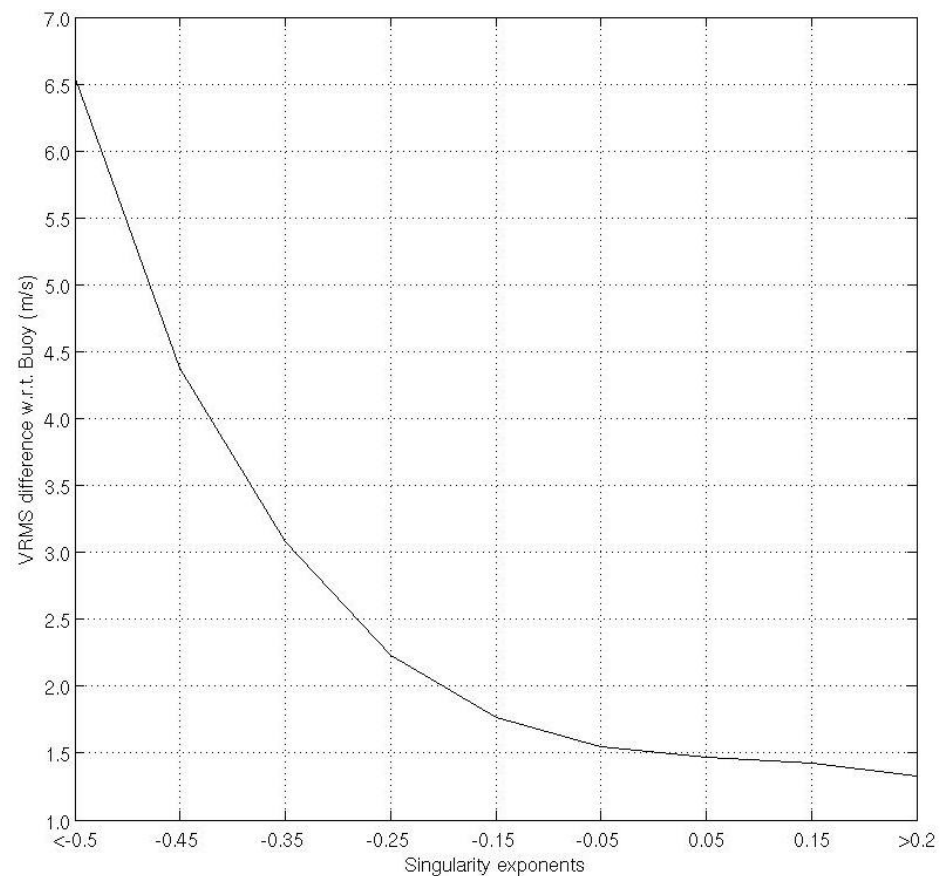


Singularity map from wind speed modified wind direction and MLE

- Most negative SE values well aligned with actual front
- Combination of speed, modified direction, and MLE seems optimal

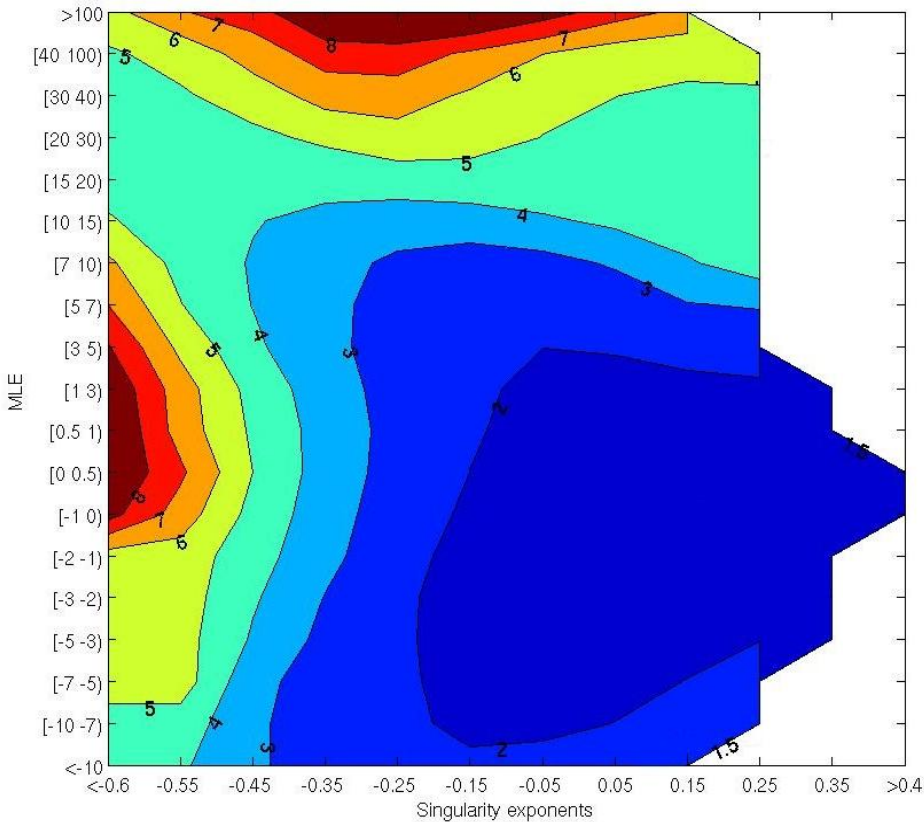


WVCs with  $SE < -0.4$   
MLE-based QC denoted by the asterisks

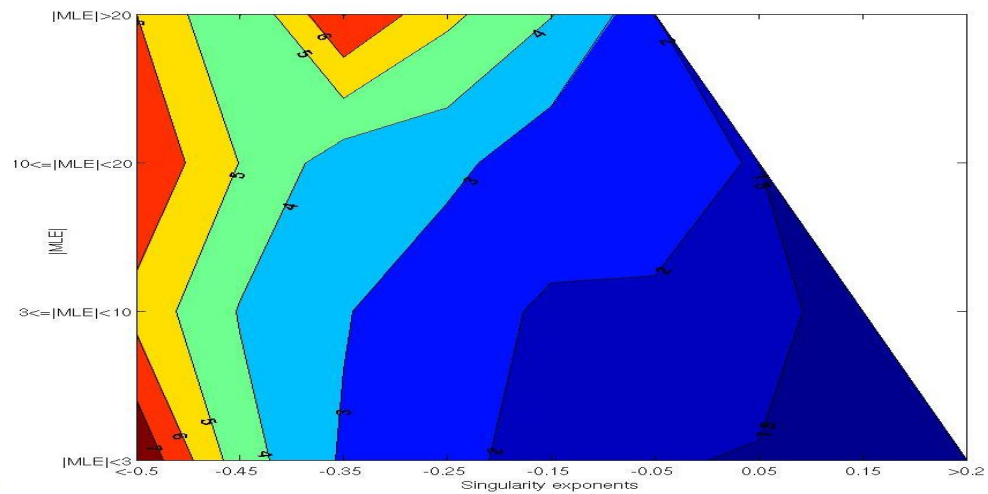


Mean Vector RMS (VRMS) difference  
between ASCAT selected solutions and  
buoy winds

- Stronger filtering of SE-based QC along front w.r.t. MLE-based QC
- Clear relation between SE value and ASCAT wind quality

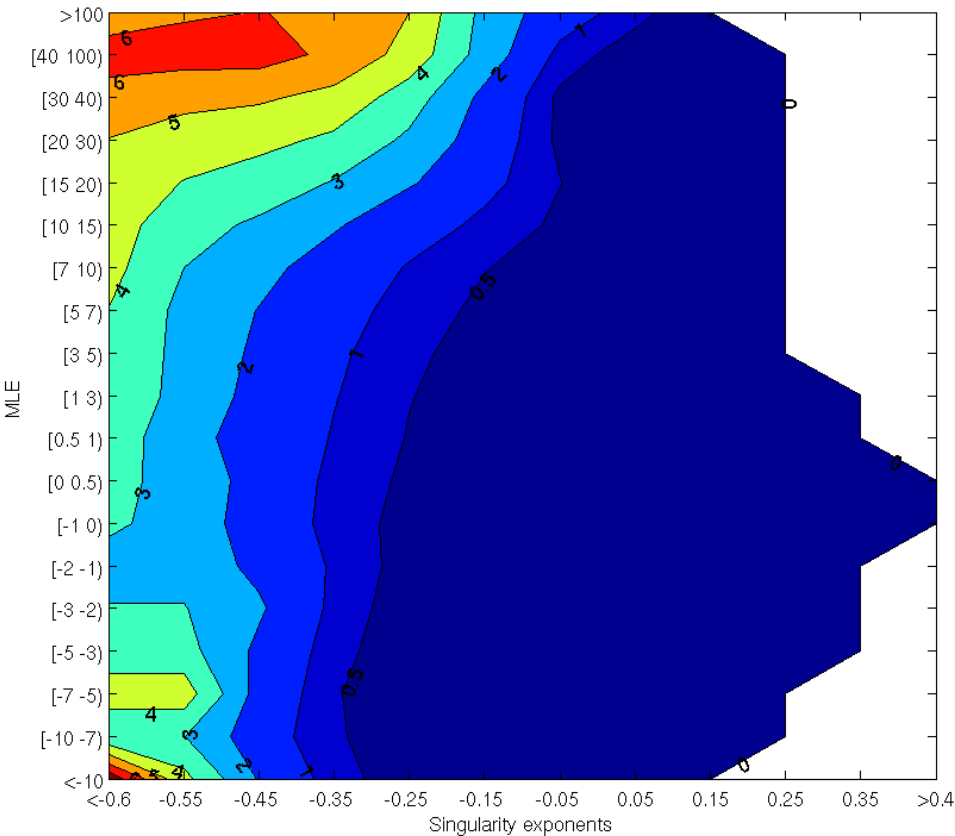


Vector RMS difference  
ASCAT-ECMWF winds (>4 m/s)

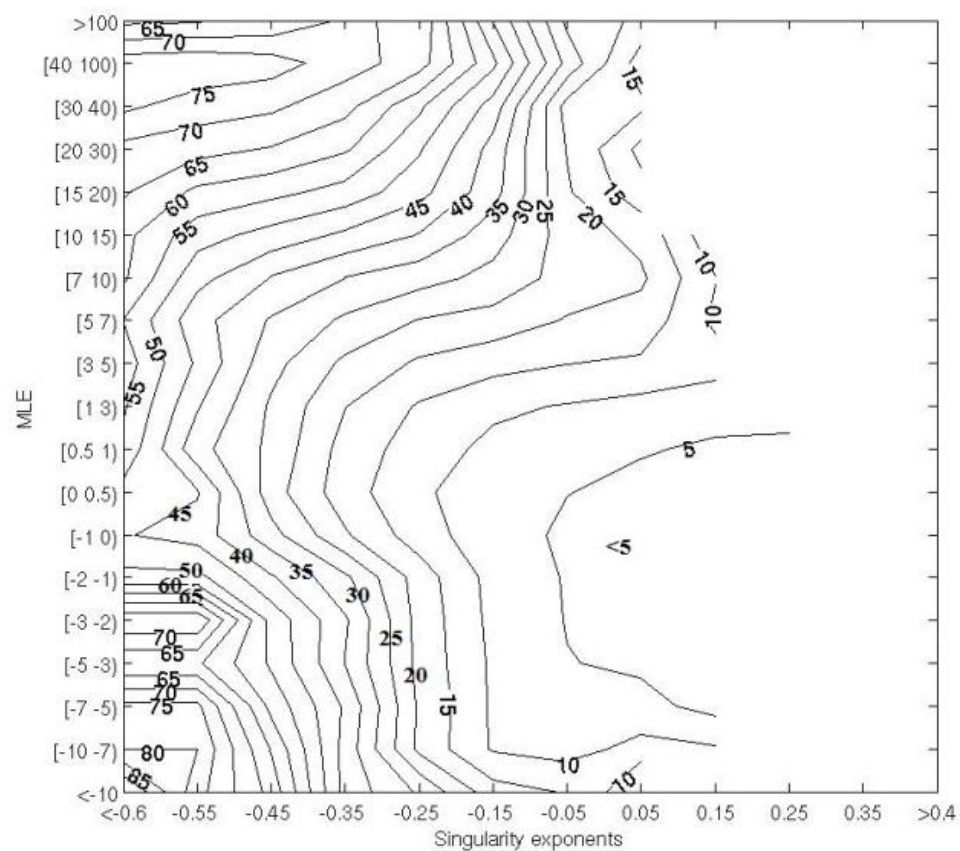


Vector RMS difference  
ASCAT-buoy winds (>4 m/s)

- **MLE-and SE-based QCs are strongly complementary**



Mean TMI RR

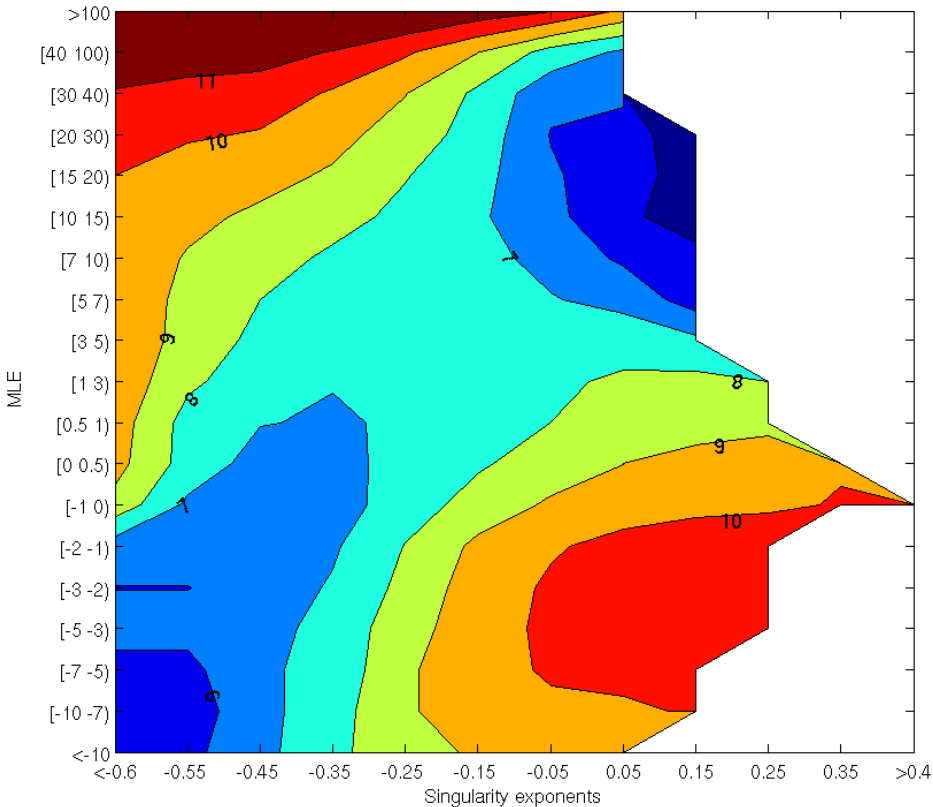


% TMI RR > 3 mm/hr

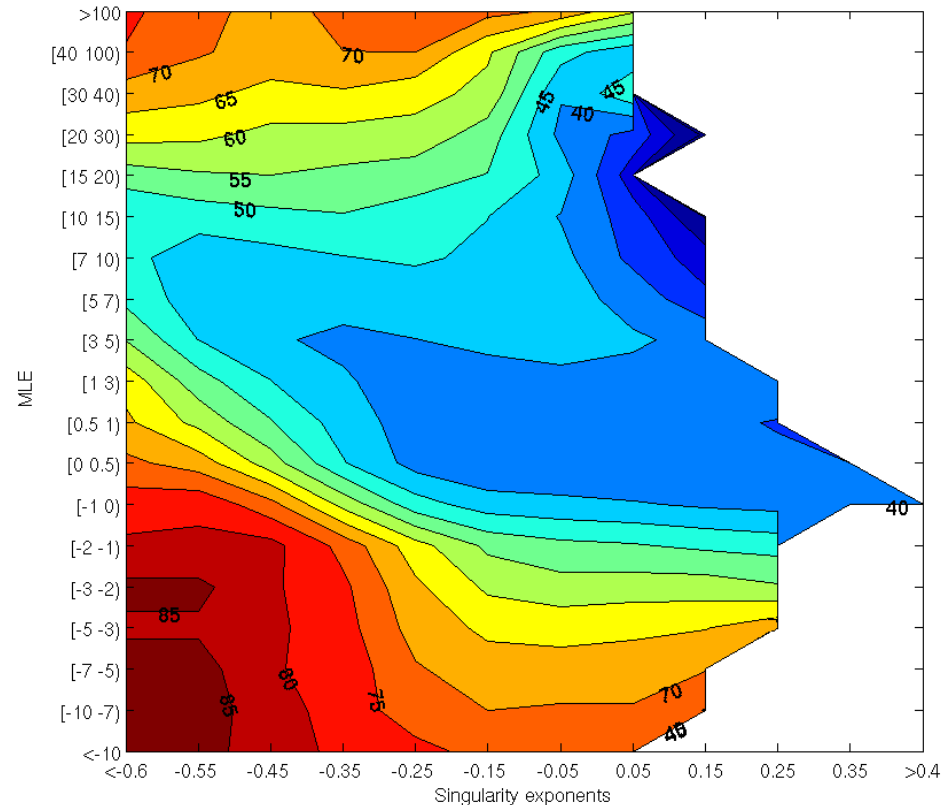
- Increasing rain contamination at decreasing SE and increasing |MLE|
- Triplets outside and far away from the cone (very negative MLEs) also contaminated (only at moderate winds)



# Only rain contaminated WVCs

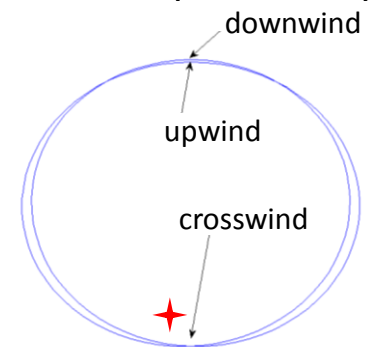


ASCAT mean wind speed (1st-rank)



ASCAT mean wind direction (1st-rank)

- At low winds, rain splashing projects triplets towards crosswind and outside the cone surface
- At high winds, splashing also projects triplets towards crosswind but stay inside the cone surface



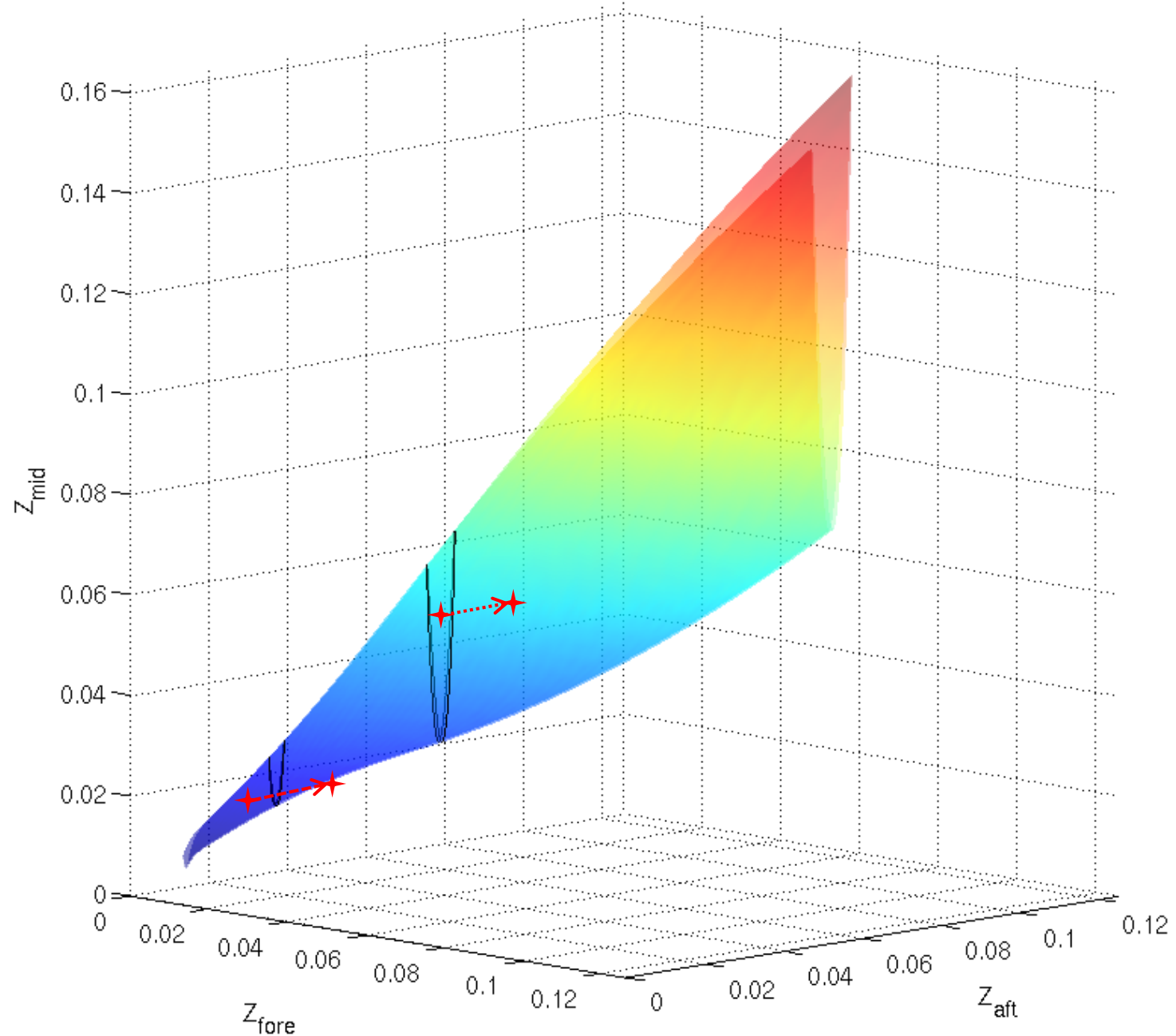


Fig.1 3D visualization of CMOD5n for WVC number 1 ( $0 \text{ m/s} < V \leq 15 \text{ m/s}$ ). The black ellipse defines the GMF for  $V = 4, 8 \text{ m/s}$  respectively

Table 2. Statistics of ASCAT ‘selected’ winds w.r.t. buoy winds as a function of SE threshold.

Criterion	VRMS/rejected WVCs	VRMS/kept WVCs	Rejecting ratio (%)
$T_{SE}=-0.40$ or $T_{MLE}=+18.6$	4.99	1.62	1.06
$T_{SE}=-0.45$ or $T_{MLE}=+18.6$	5.63	1.63	0.66
$T_{MLE}=+18.6$	5.43	1.65	0.34

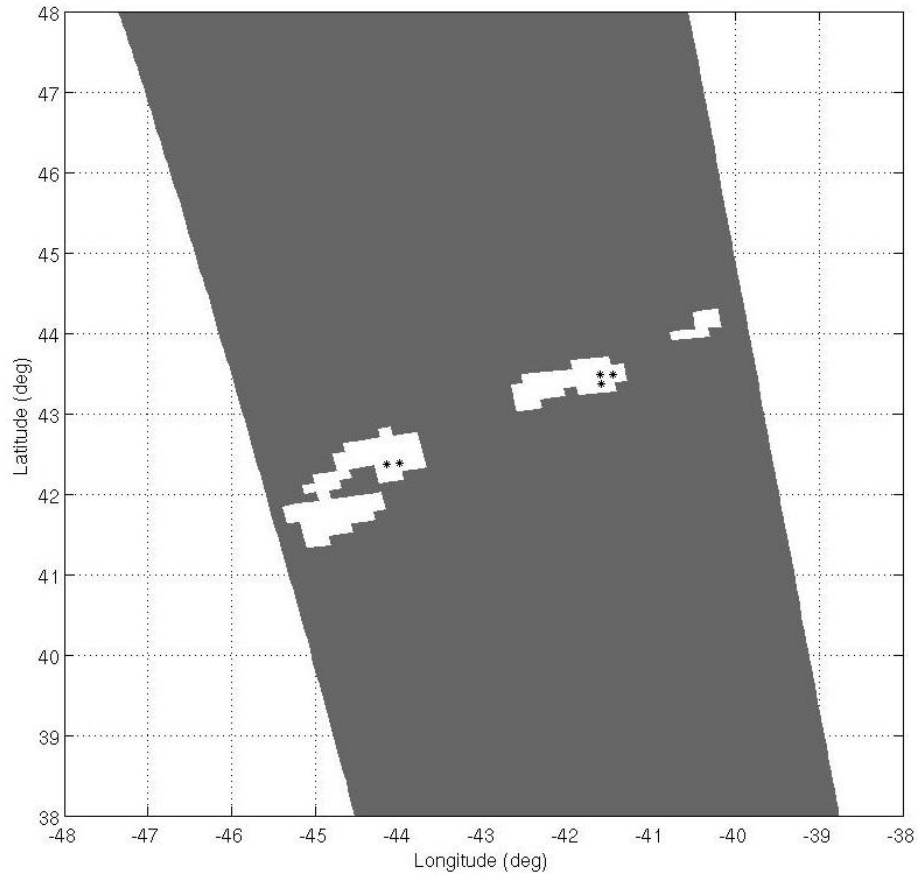
# Conclusions

- Singularity analysis (SA) is a powerful tool to detect rain contamination and in general poor quality retrievals
- SA is complementary to MLE-based QC
- SA can be used to detect 2D-VAR ambiguity removal errors (e.g., ASCAT-retrieved spurious wind fronts)
- Future work
  - To use NEXRAD data
  - To explore Kp information content
  - To implement an improved ASCAT QC in AWDP
  - To develop a rain-correction model
  - To apply these techniques to ASCAT-B, OSCAT, HY-2<sup>a</sup>, etc.
- *A singularity map service will soon be available at:*  
**<http://cp34-bec.cmima.csic.es>**

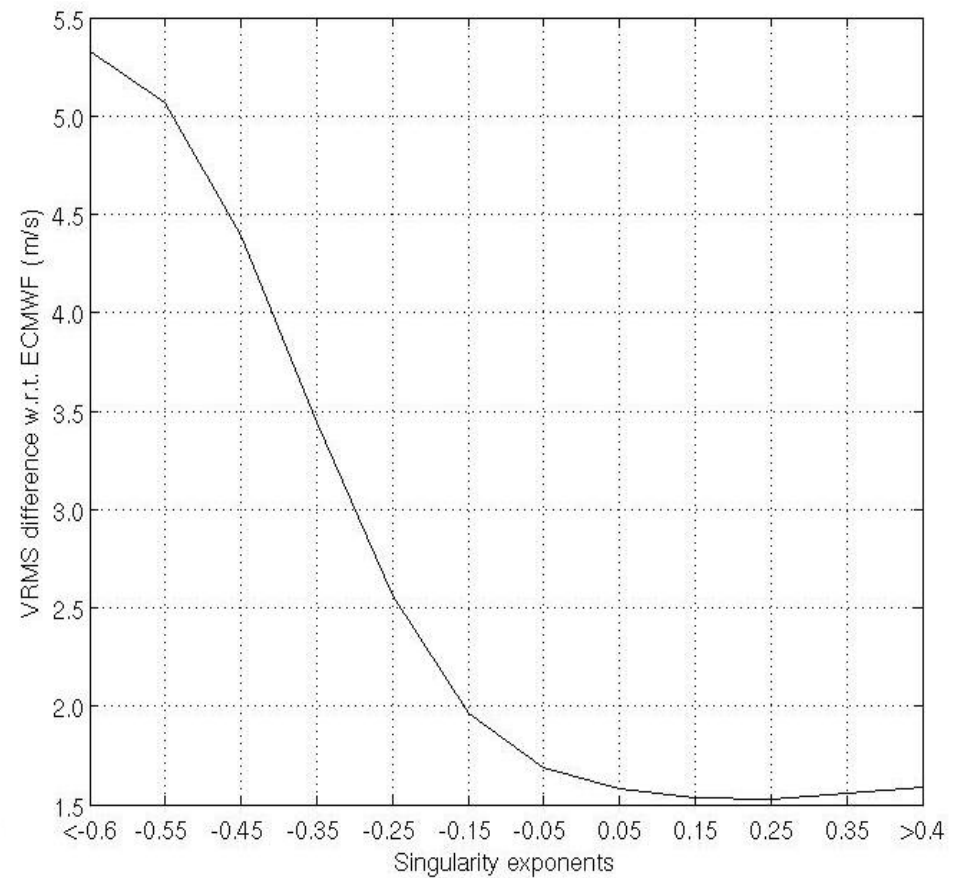


### 3. SA application

- Before, it showed that the lowest (most negative) singularity exponent values for one of the zonal (U) and meridional (V) wind components were good choice for revealing the artefacts associated with the ASCAT measurements. <---Spurious wind front
- Now, singularity maps of MLE and the retrieved wind components (speed and direction) are examined independently for the particular wind field case. Then at every grid point, the minimum SE value from the wind speed, wind direction and MLE is used to generate the unique singularity map.



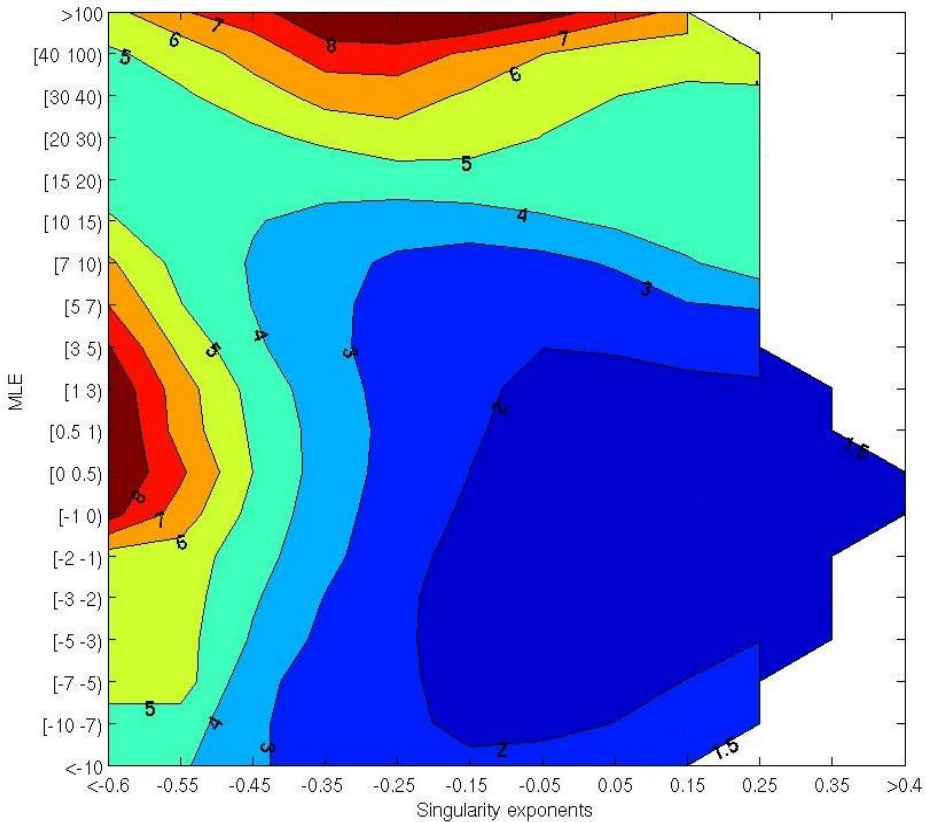
WVCs with  $SE < -0.4$ . MLE-based QC denoted by the asterisks.



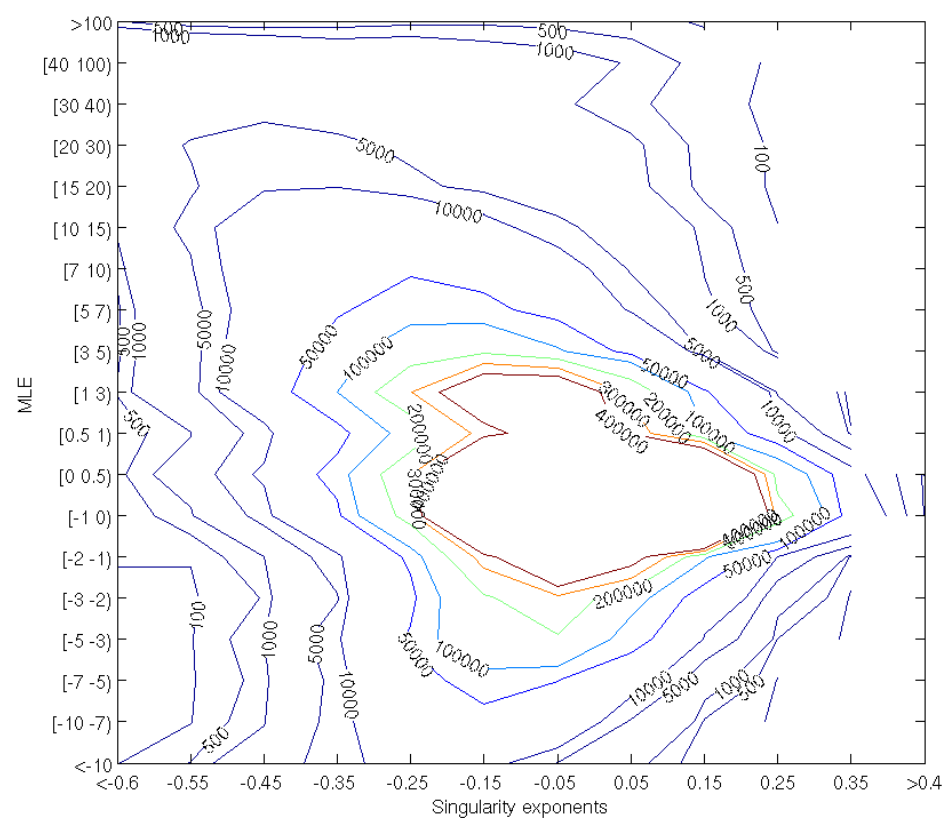
Mean Vector RMS (VRMS) difference between ASCAT selected solutions and ECMWF winds

Table 1. Statistics of ASCAT ‘selected’ winds w.r.t. ECMWF as a function of SE threshold. The second row presents the VRMS difference for the rejected WVCs, the third row shows the VRMS difference for the kept WVCs, and the last row indicates the number of rejected WVCs. For comparison, the last column presents the result corresponding to the current operational QC.

SE threshold	-0.6	-0.5	-0.4	-0.3	-0.2	MLE>+18.6
VRMS/Rejected	5.34	5.14	4.59	3.77	2.94	5.39
VRMS/Kept	1.78	1.78	1.76	1.73	1.68	1.77
Rejecting ratio(%)	0.053	0.20	0.74	2.56	8.19	0.28



Vector RMS difference  
ASCAT-ECMWF winds (>4 m/s)



Vector RMS difference  
ASCAT-ECMWF winds (>4 m/s)



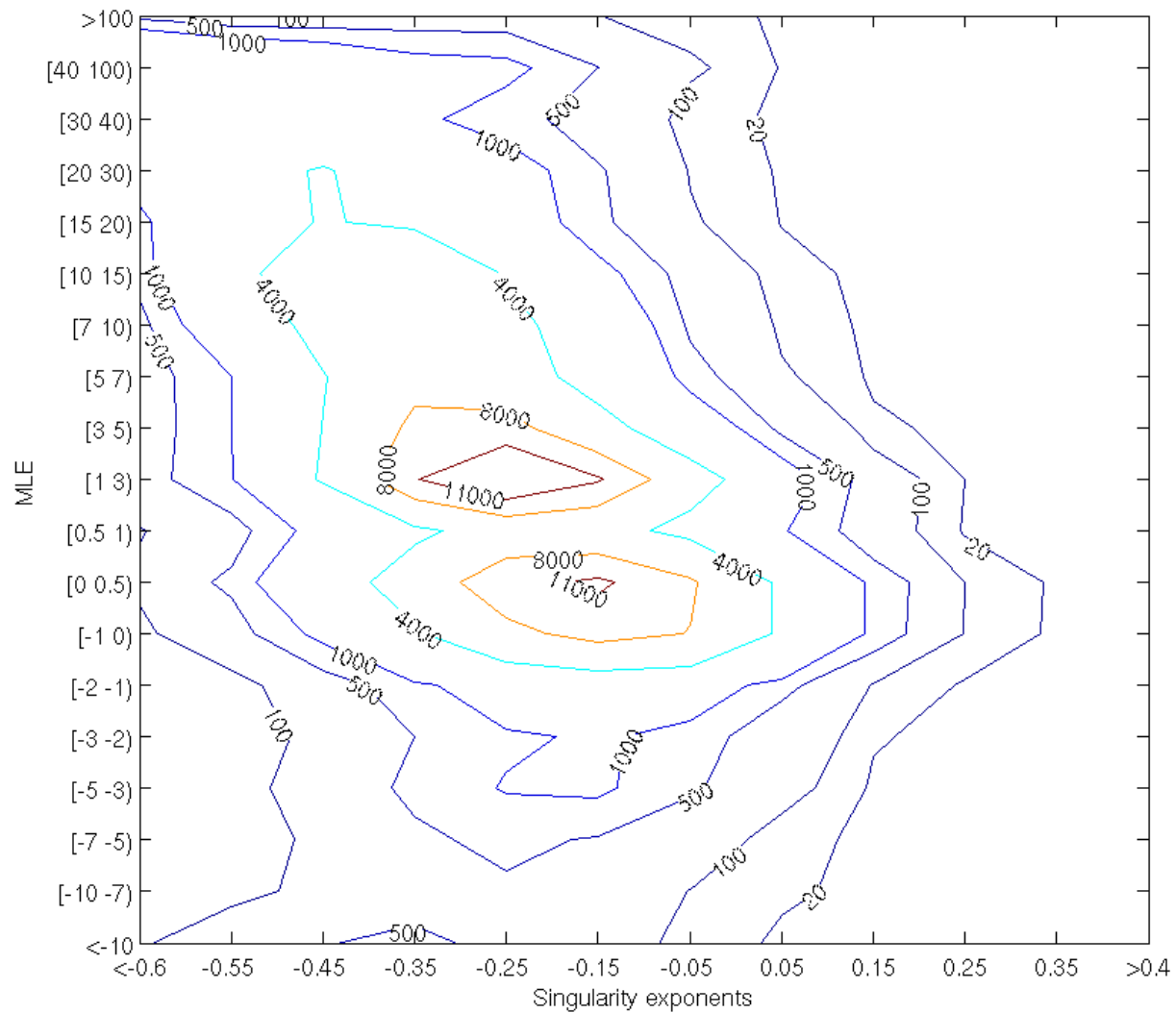


Fig. 12 (additional). Contour plot of the number of WVCs with TMI-RR>3 mm/hr in 2D-bins. (WVCs with speed>4 m/s are considered. Indeed, nearly none of WVC with speed<4m/s is collocated with RR>3 mm/hr).

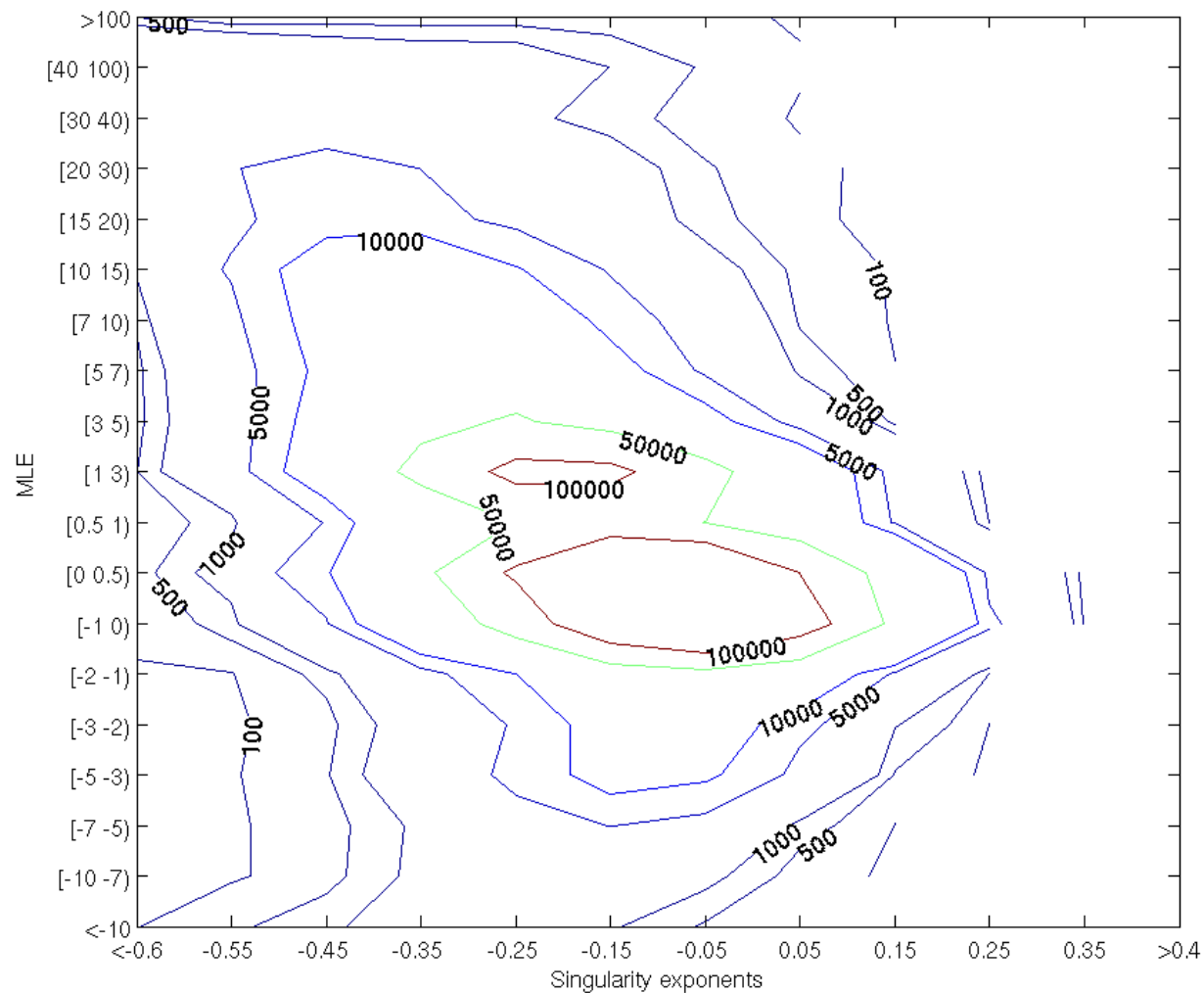
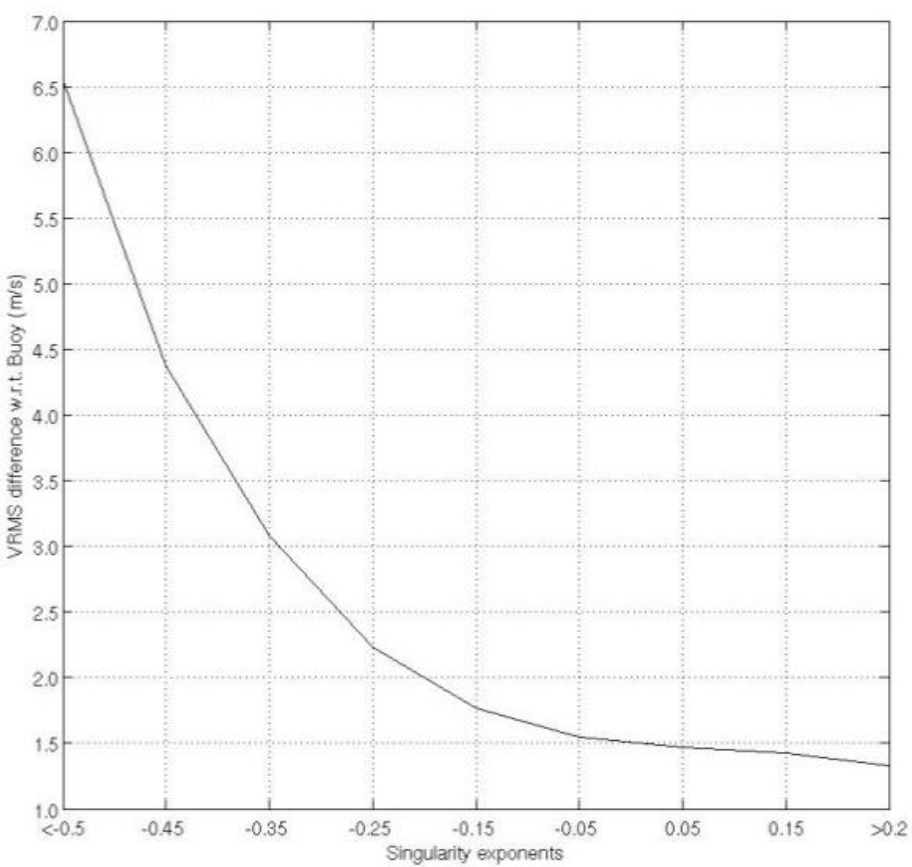
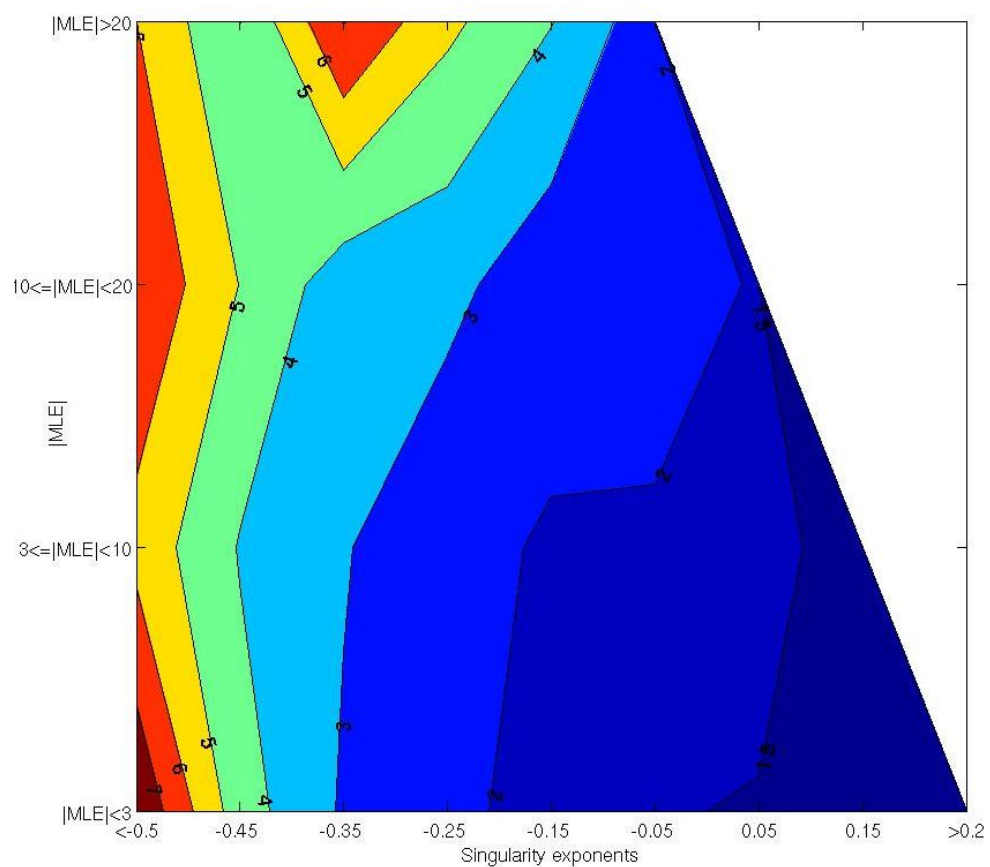


Fig. 12 (additional). Contour plot of the number of WVCs with TMI-RR>0 mm/hr in 2D-bins. (All speed regions are considered)



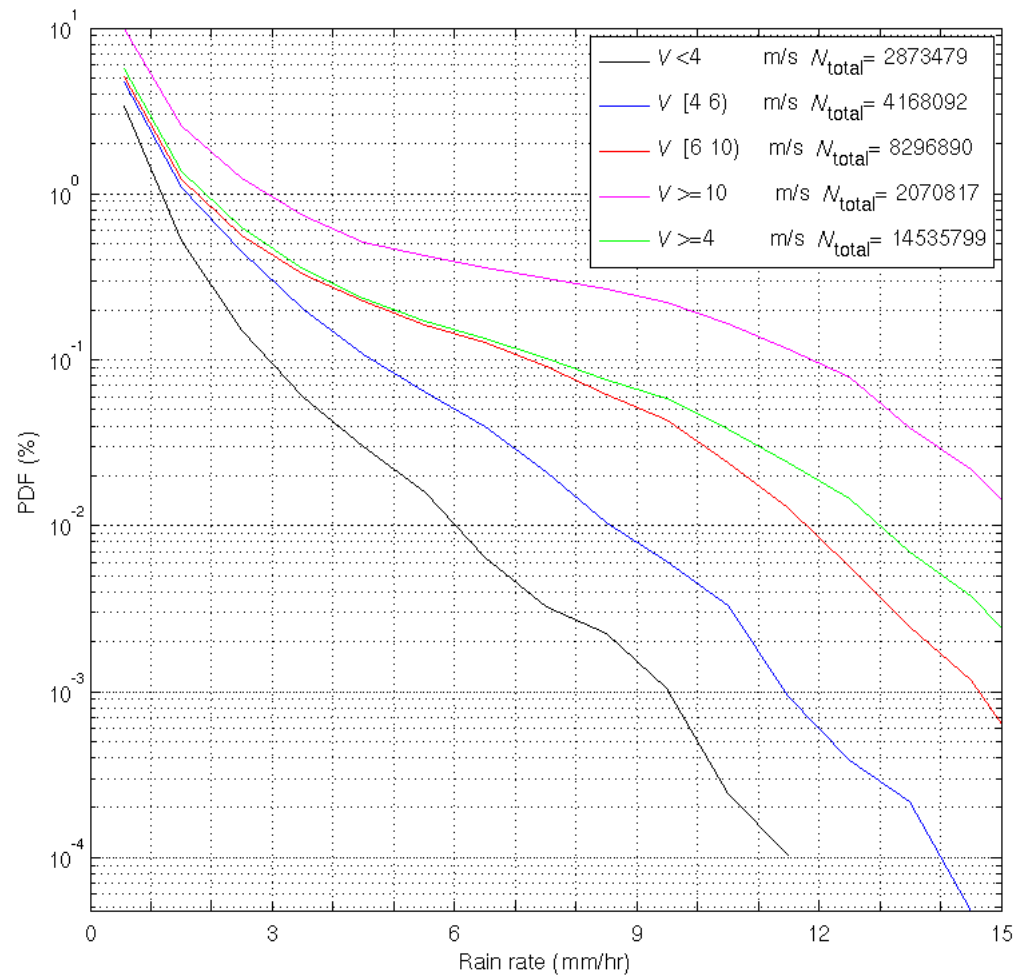
(a)



(b)

Fig. 14. The mean VRMS difference w.r.t. buoy as a function of (a) singularity exponents and (b) for different  $|MLE|$

# Rain histogram in different wind regions



RR histogram in different wind regions. The legend shows the total number of WVCs in each speed category



# Rain identification (Comparison among singularity exponent, MLE and Kp, separating into different wind regions )

**4 m/s  $\leq$  Wind speed < 6 m/s**

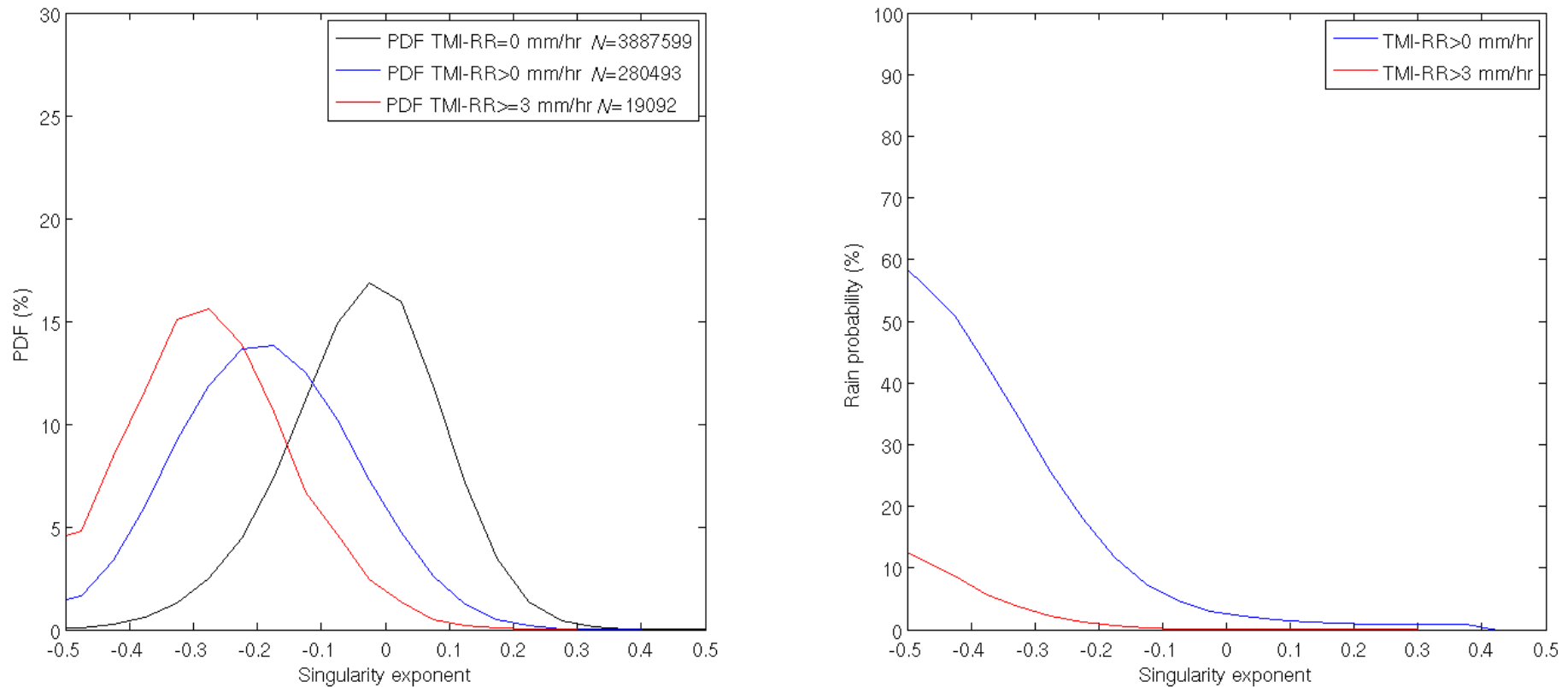


Fig. 1. (left panel) the histogram of WVCs in terms of singularity exponents, black line: all wvcs, blue line: wvcs with collocated TMI-RR>0 mm/hr, red line: wvcs with TMI-RR>=3 mm/hr. (right panel) the rain probability as a function of singularity exponent.

# Rain identification (Comparison among singularity exponent, MLE and Kp, separating into different wind regions )

**Wind speed  $\geq 10$  m/s**

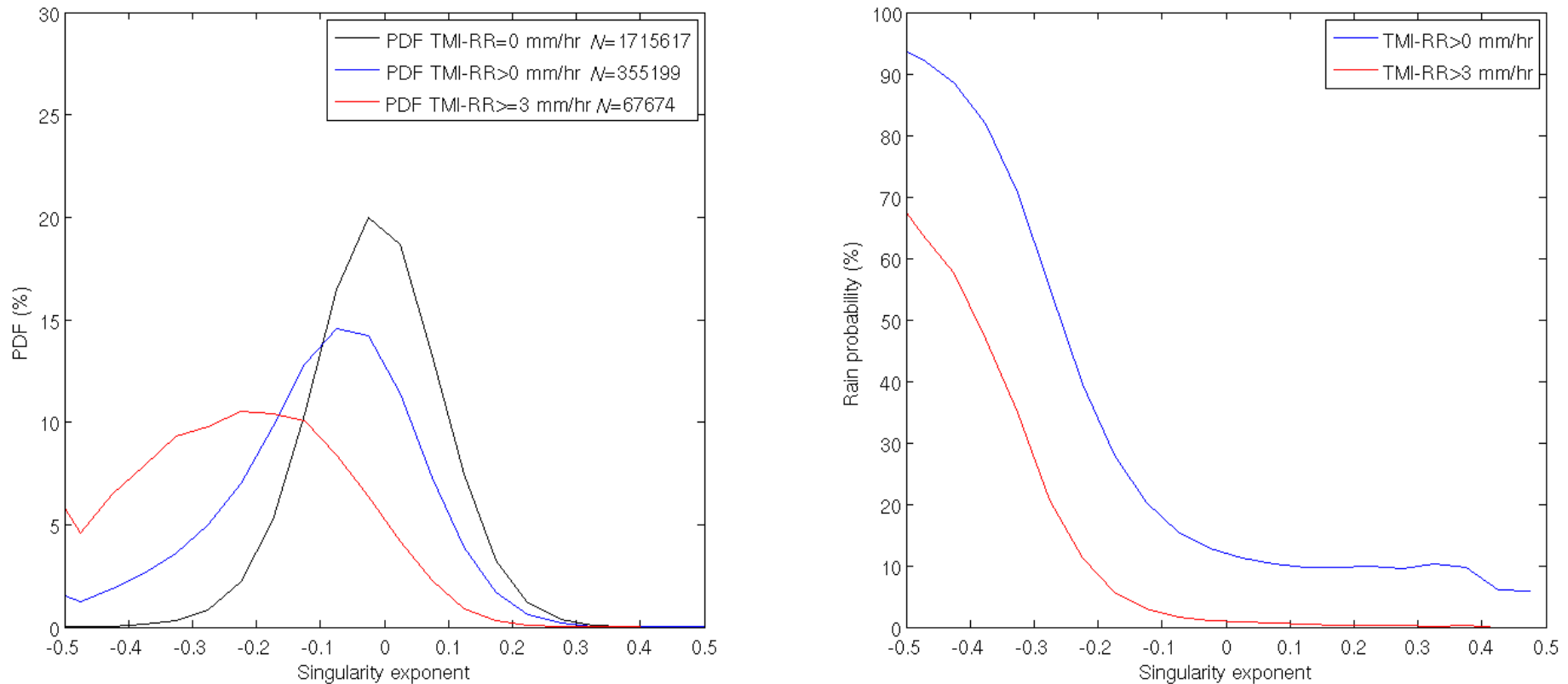


Fig. 2. (left panel) the histogram of WVCs in terms of singularity exponents, black line: all wvcs, blue line: wvcs with collocated TMI-RR>0 mm/hr, red line: wvcs with TMI-RR>=3 mm/hr. (right panel) the rain probability as a function of singularity exponent.

# Rain identification (Comparison among singularity exponent, MLE and Kp, separating into different wind regions )

**Wind speed  $\geq 4$  m/s**

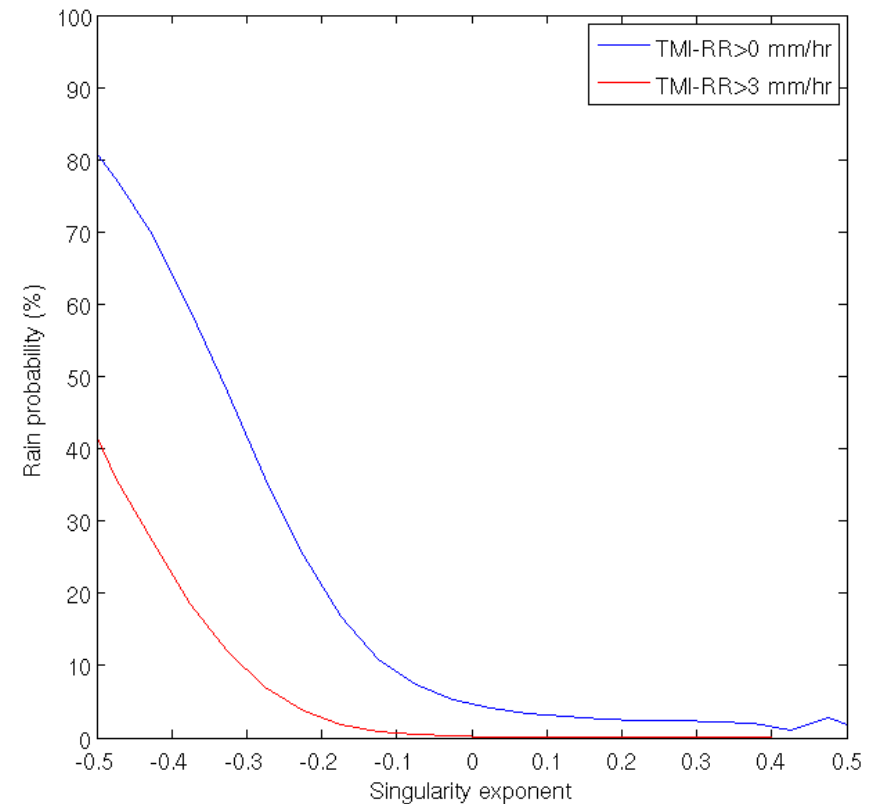
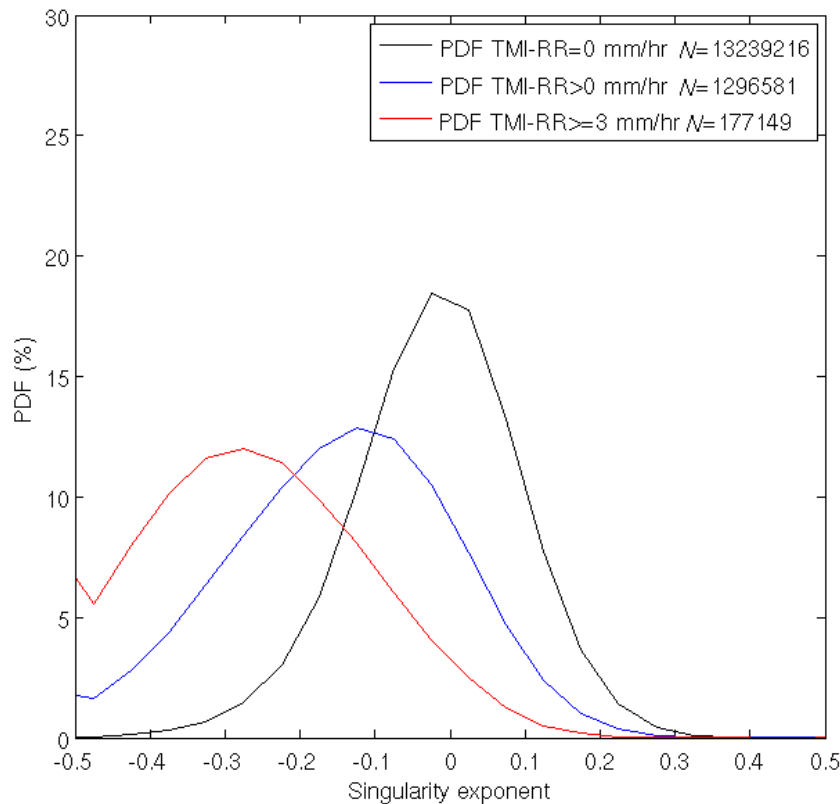


Fig. 3. (left panel) the histogram of WVCs in terms of singularity exponents, black line: all wvcs, blue line: wvcs with collocated TMI-RR>0 mm/hr, red line: wvcs with TMI-RR>=3 mm/hr. (right panel) the rain probability as a function of singularity exponent.

# Rain identification (Comparison among singularity exponent, MLE and Kp, separating into different wind regions )

**4 m/s  $\leq$  Wind speed < 6 m/s**

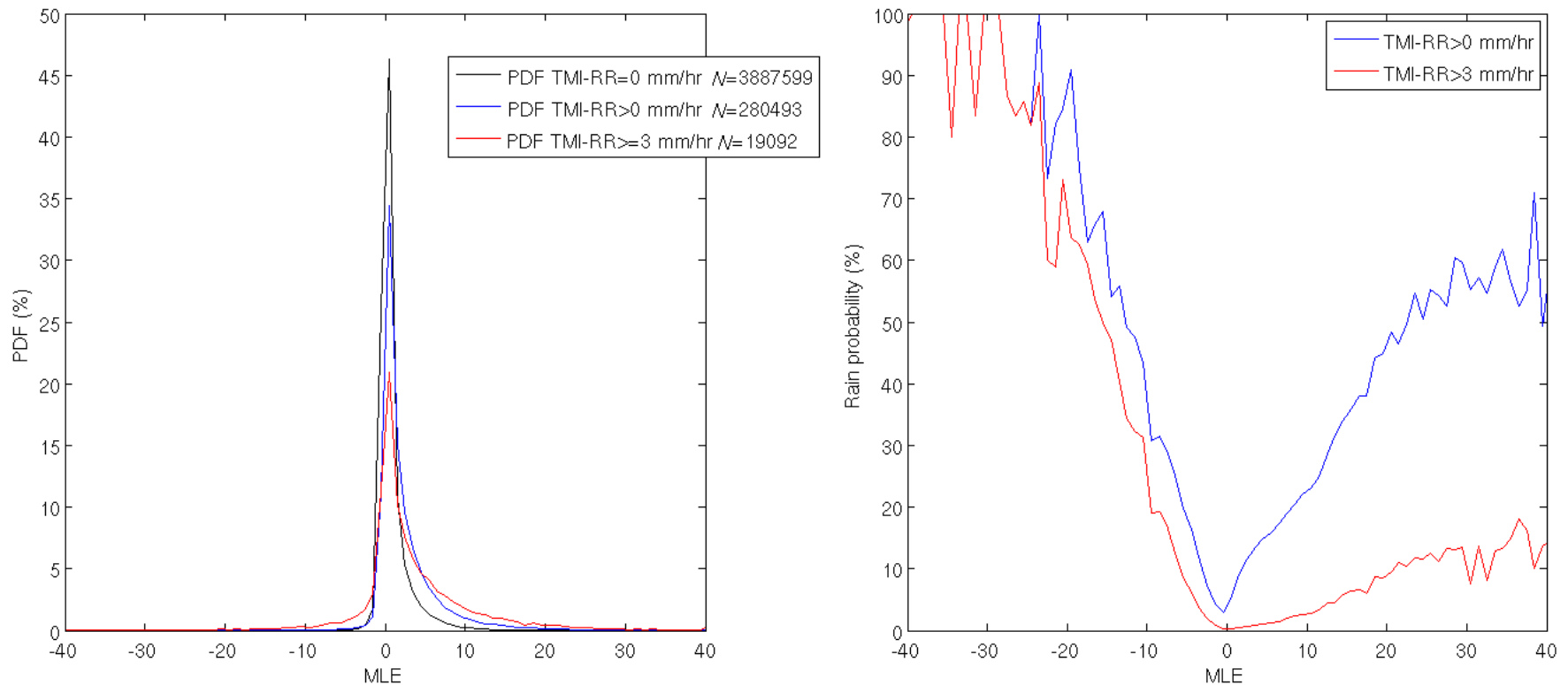


Fig. 4. (left panel) the histogram of WVCs in terms of MLE, black line: all wvcs, blue line: wvcs with collocated TMI-RR>0 mm/hr, red line: wvcs with TMI-RR>=3 mm/hr. (right panel) the rain probability as a function of singularity exponent.

# Rain identification (Comparison among singularity exponent, MLE and Kp, separating into different wind regions )

**Wind speed  $\geq 10$  m/s**

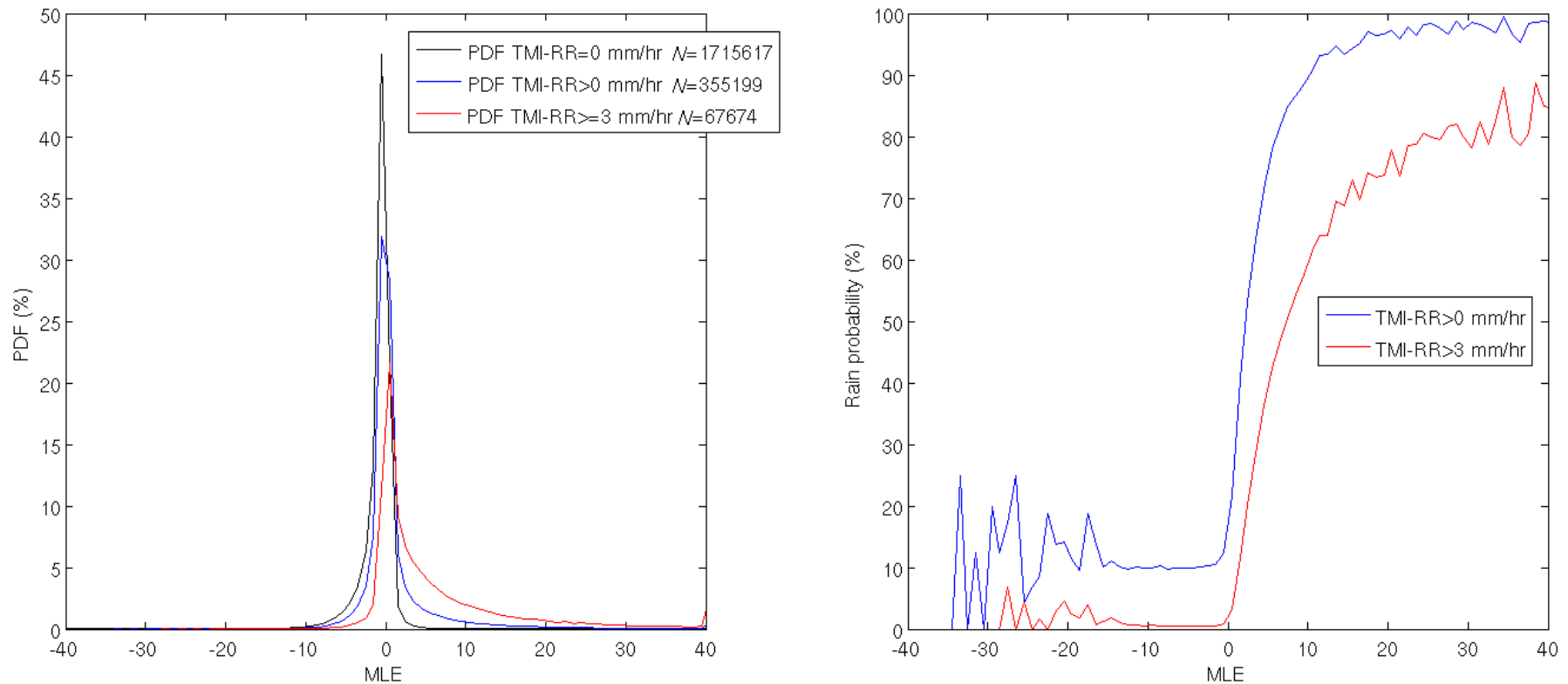


Fig. 5. (left panel) the histogram of WVCs in terms of MLE, black line: all wvcs, blue line: wvcs with collocated TMI-RR>0 mm/hr, red line: wvcs with TMI-RR $\geq$ 3 mm/hr. (right panel) the rain probability as a function of singularity exponent.

# Rain identification (Comparison among singularity exponent, MLE and Kp, separating into different wind regions )

**Wind speed  $\geq 4$  m/s**

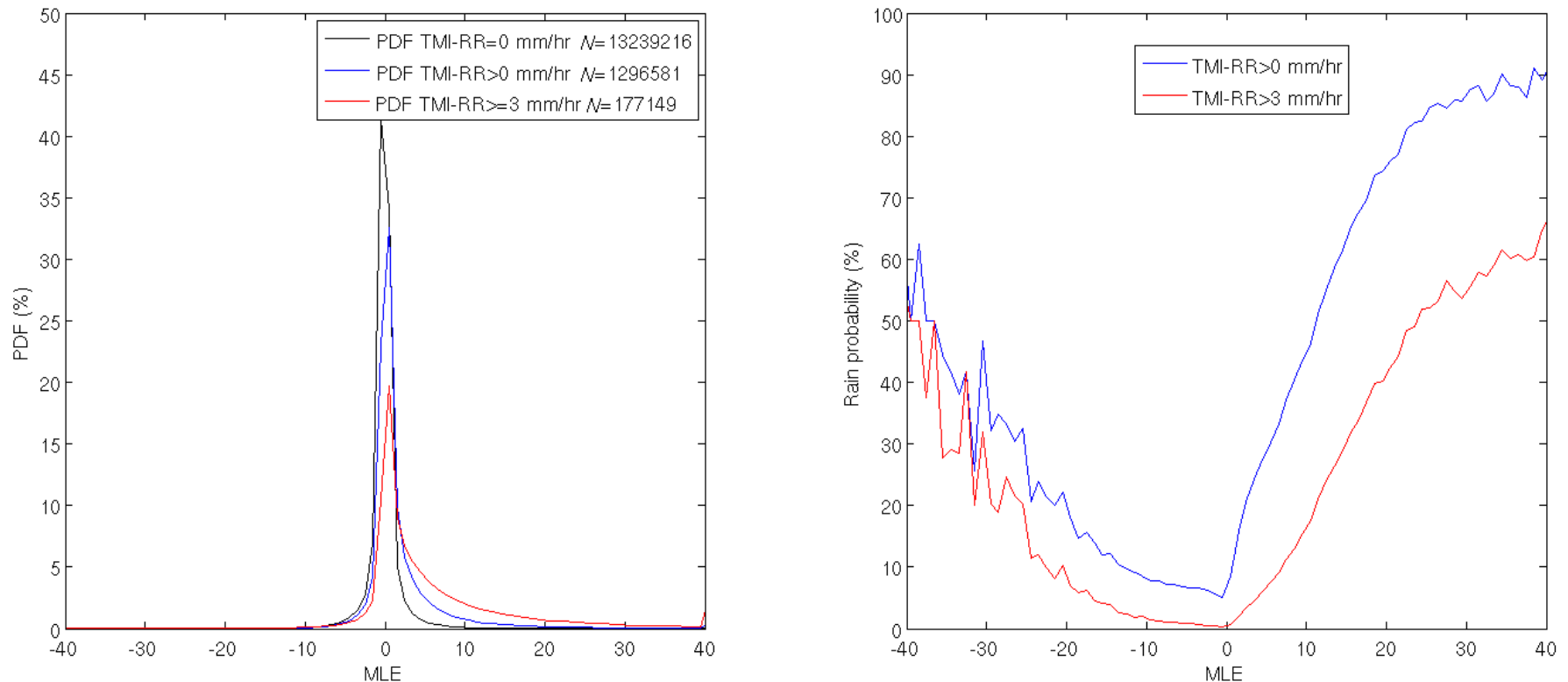


Fig. 6. (left panel) the histogram of WVCs in terms of MLE, black line: all wvcs, blue line: wvcs with collocated TMI-RR>0 mm/hr, red line: wvcs with TMI-RR>=3 mm/hr. (right panel) the rain probability as a function of singularity exponent.



# Rain identification (Comparison among singularity exponent, MLE and Kp, separating into different wind regions )

**4 m/s  $\leq$  Wind speed < 6 m/s**

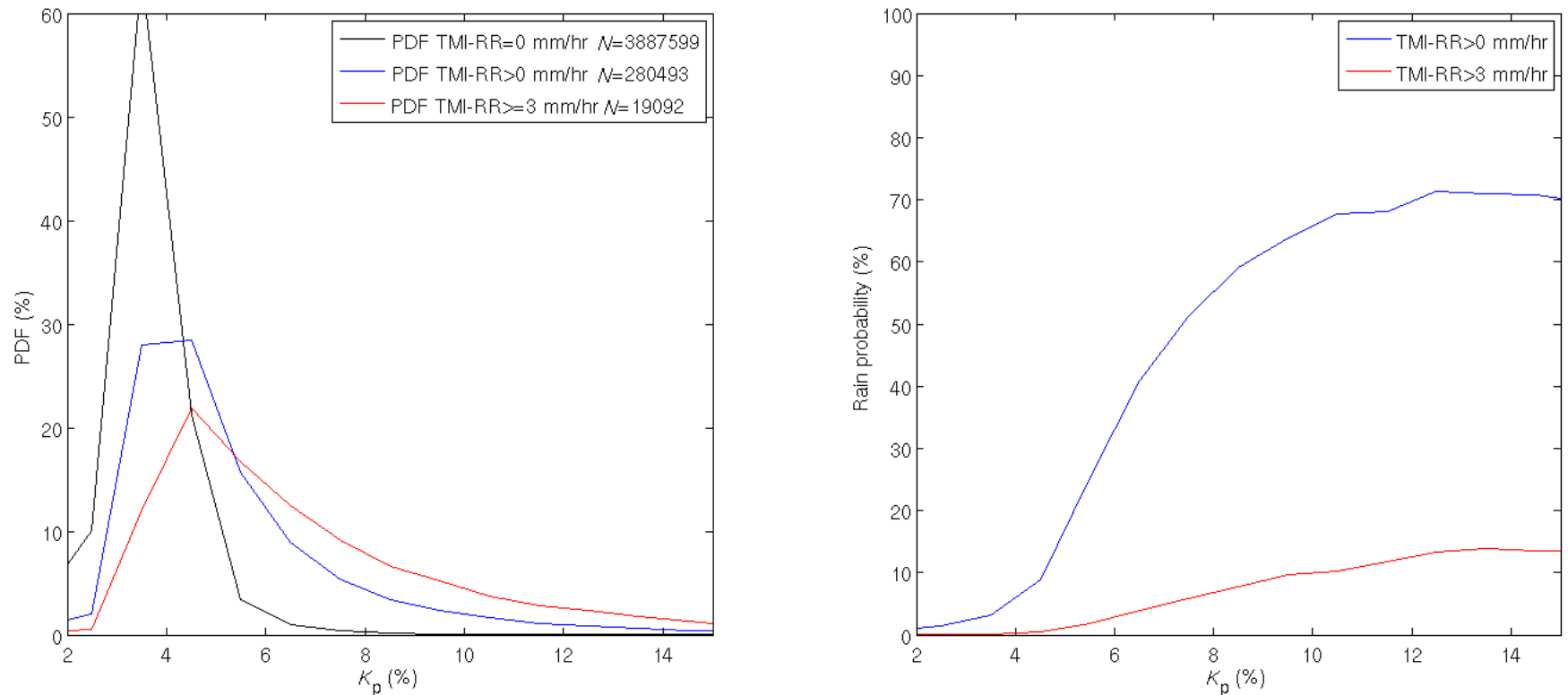


Fig. 7. (left panel) the histogram of WVCs in terms of  $K_p$ , black line: all wvcs, blue line: wvcs with collocated TMI-RR > 0 mm/hr, red line: wvcs with TMI-RR  $\geq$  3 mm/hr. (right panel) the rain probability as a function of singularity exponent.

# Rain identification (Comparison among singularity exponent, MLE and Kp, separating into different wind regions )

**Wind speed  $\geq 10$  m/s**

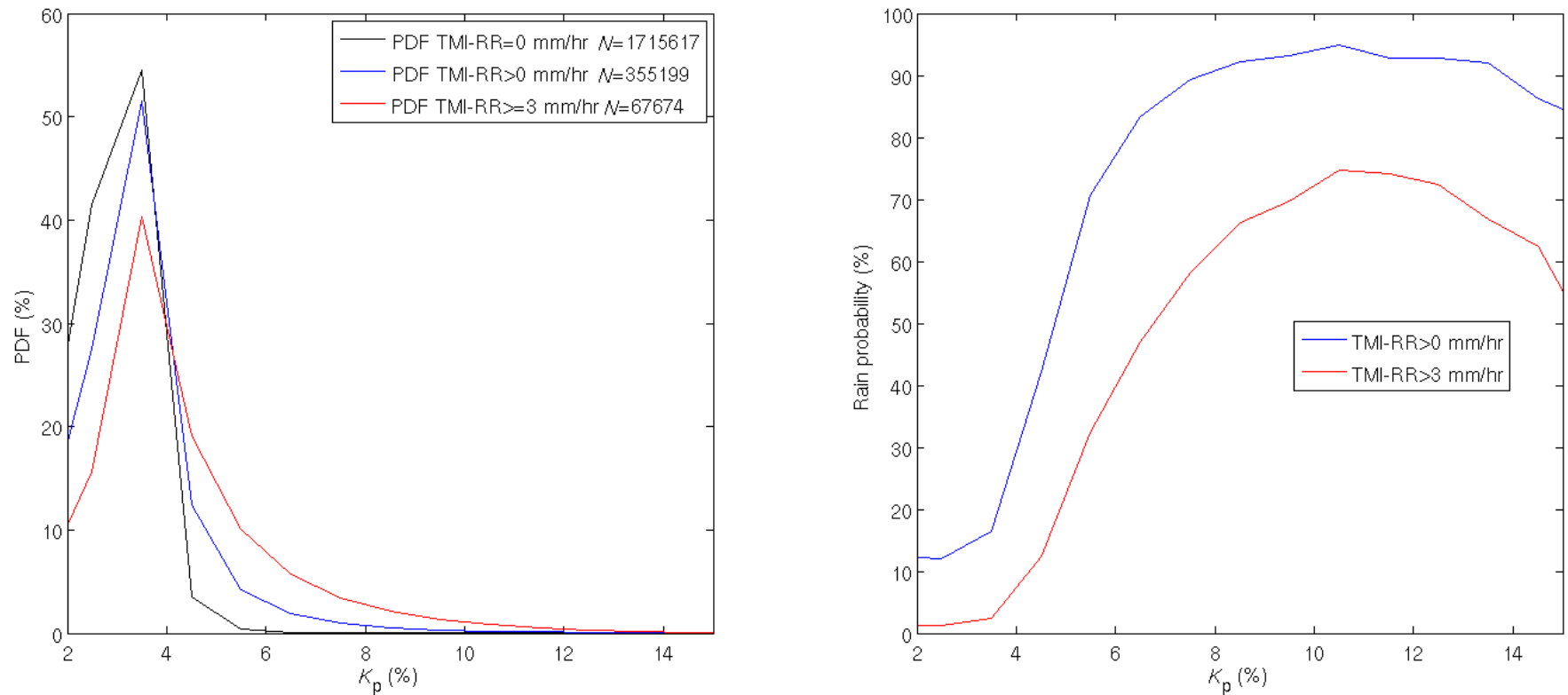


Fig. 8. (left panel) the histogram of WVCs in terms of  $K_p$ , black line: all wvcs, blue line: wvcs with collocated  $\text{TMI-RR} > 0$  mm/hr, red line: wvcs with  $\text{TMI-RR} \geq 3$  mm/hr. (right panel) the rain probability as a function of singularity exponent.

# Rain identification (Comparison among singularity exponent, MLE and Kp, separating into different wind regions )

**Wind speed  $\geq 4$  m/s**

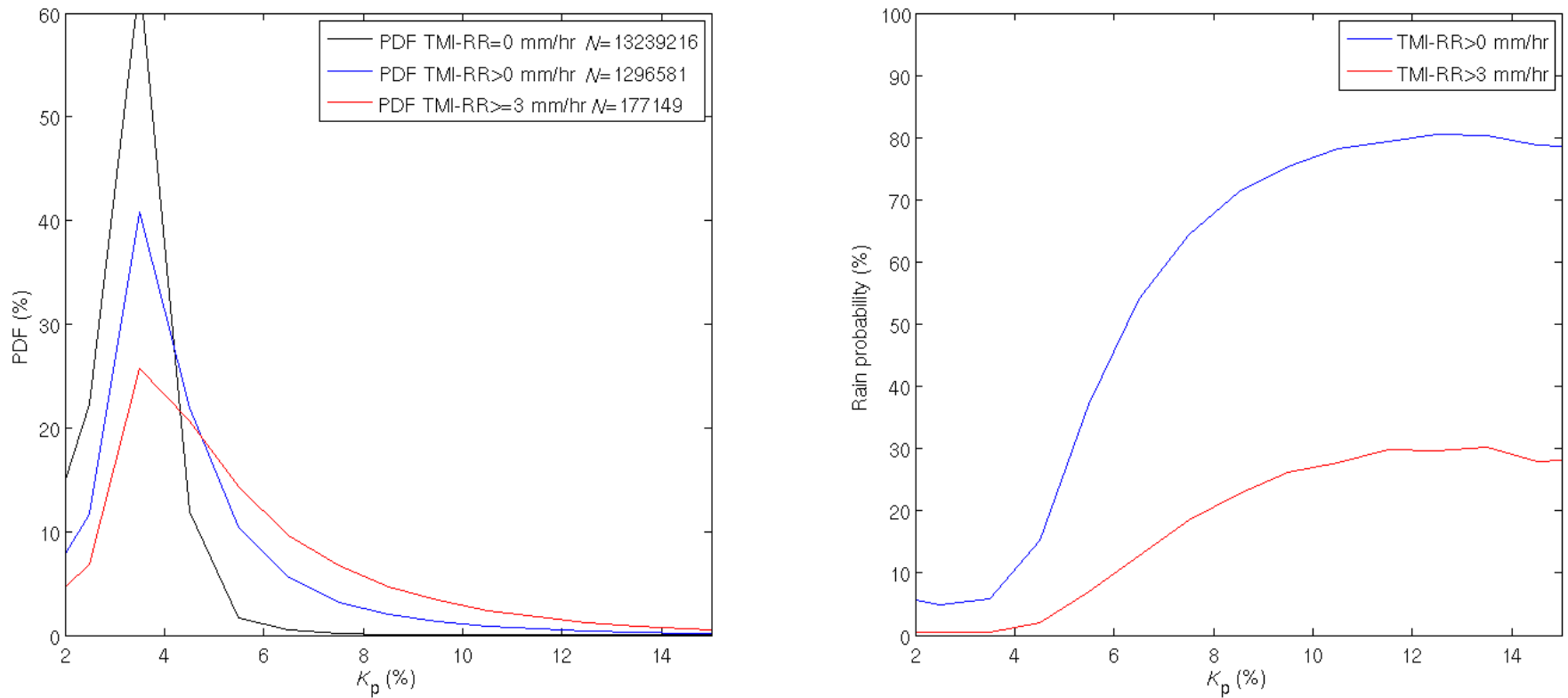


Fig. 9. (left panel) the histogram of WVCs in terms of  $K_p$ , black line: all wvcs, blue line: wvcs with collocated  $\text{TMI-RR} > 0$  mm/hr, red line: wvcs with  $\text{TMI-RR} \geq 3$  mm/hr. (right panel) the rain probability as a function of singularity exponent.

# Rain identification (Comparison among singularity exponent, MLE and $K_p$ , separating into different wind regions )

## Short comments:

For rain identification, both the PDF of rainy/rain-free WVCs and the rain probability distribution are important. To achieve an accuracy rain flag, the following two elements are desired:

1. Given a rain-sensitive parameter, the larger discrepancy between the PDFs of rainy and rain-free wvcs, the easier rain identification is.
2. The rain probability as a function of rain-sensitive parameter had better behave a 'jump' characteristic, see Figure 5. Then it is easy to set a threshold to identify rain-contaminated WVCs.

## Wind variability under rainy conditions

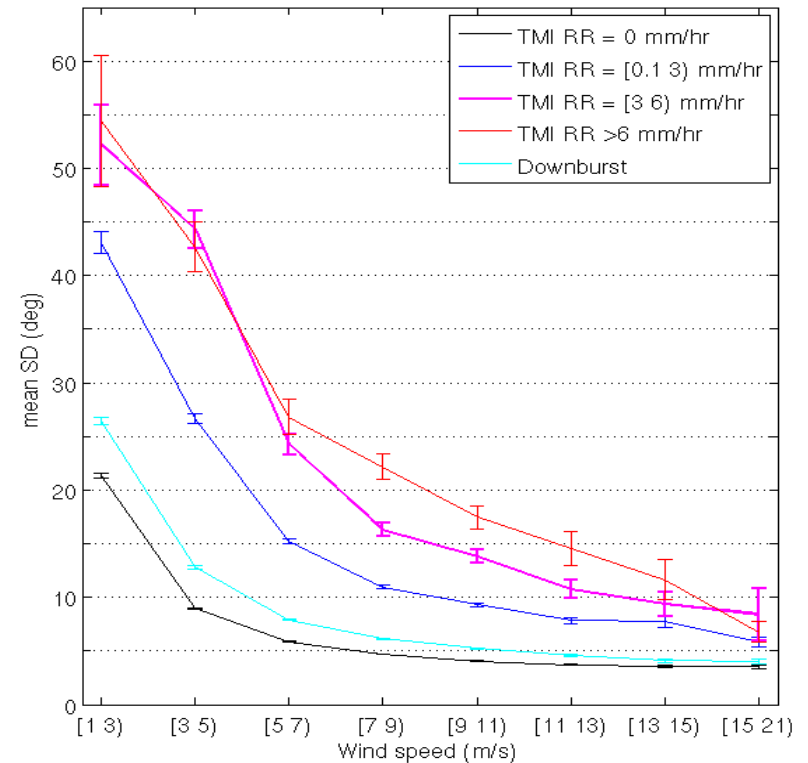
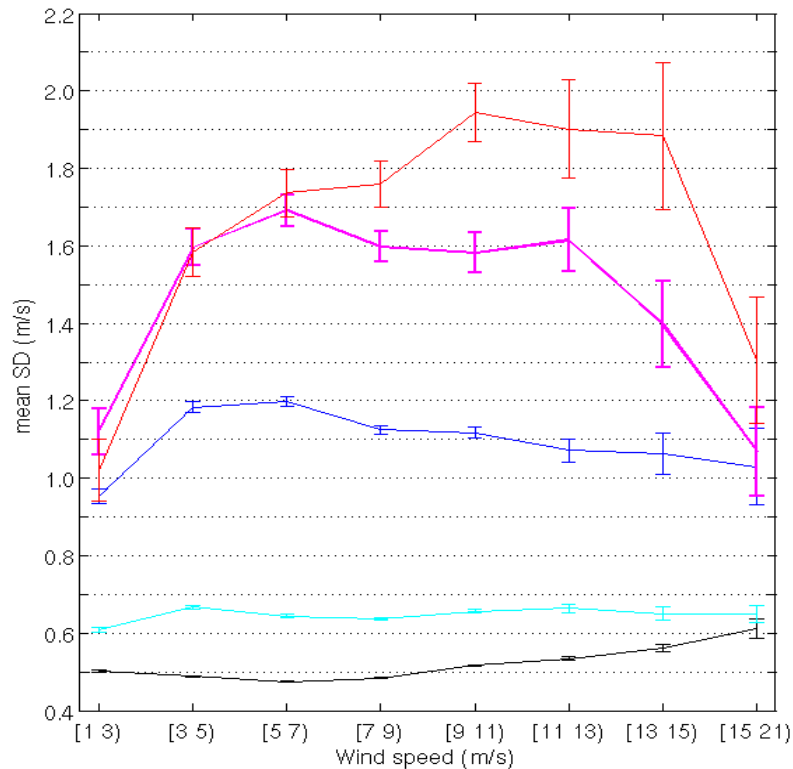
- To date, it is still a challenge to model the rain-induced surface perturbation backscatter. Through studying the rain-induced wind variability, the former factor may be estimated more accurately by subtracting the contribution(s) of wind variability (and perhaps rain-induced atmospheric backscatter) from the total backscatter.

# Wind variability under rainy conditions

- The data set consists of six years of TRMM/TMI rain data (from January 2007 to December 2012) collocated with ten-minute average buoy wind records. The collocation criteria for buoy data are less than 60-min time and  $0.25^\circ$  spatial distance from the TMI measurement. Therefore, a sequence of 25 buoy samples is recorded for each individual collocation. The 13<sup>th</sup> buoy measurement is within 5-min w.r.t. TMI measurement. Meanwhile, for each collocated TMI measurement, the neighbor eight cells of rain data are also recorded in the data set. There is a total amount of about 150 thousands collocations.
- To study the rain-induced wind variability, these data are separated into five categories, i.e.,
- C1:  $3 \times 3$  TMI grids are all rain free;
- C2: the center TMI grid is rain free, but there are rainy measurements in its neighbors; (downburst?)
- C3: the center TMI RR  $[0.1 \ 3)$  mm/hr;
- C4: the center TMI RR  $[3 \ 6)$  mm/hr;
- C5: the center TMI  $RR \geq 6$  mm/hr;
- The number of collocations in each category is 105 thousands, 38 thousands, 11 thousands, 1260 and 664 respectively.

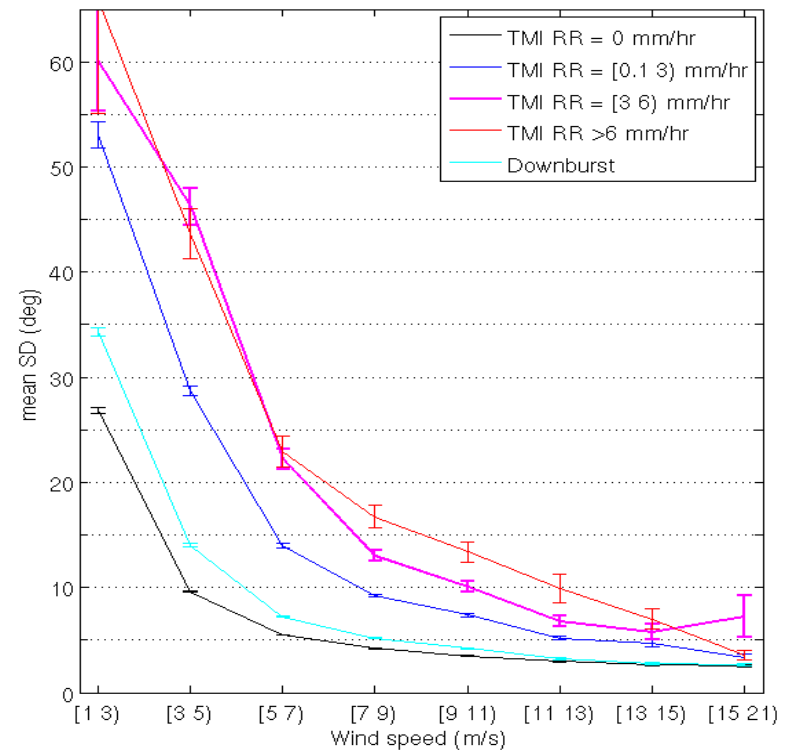
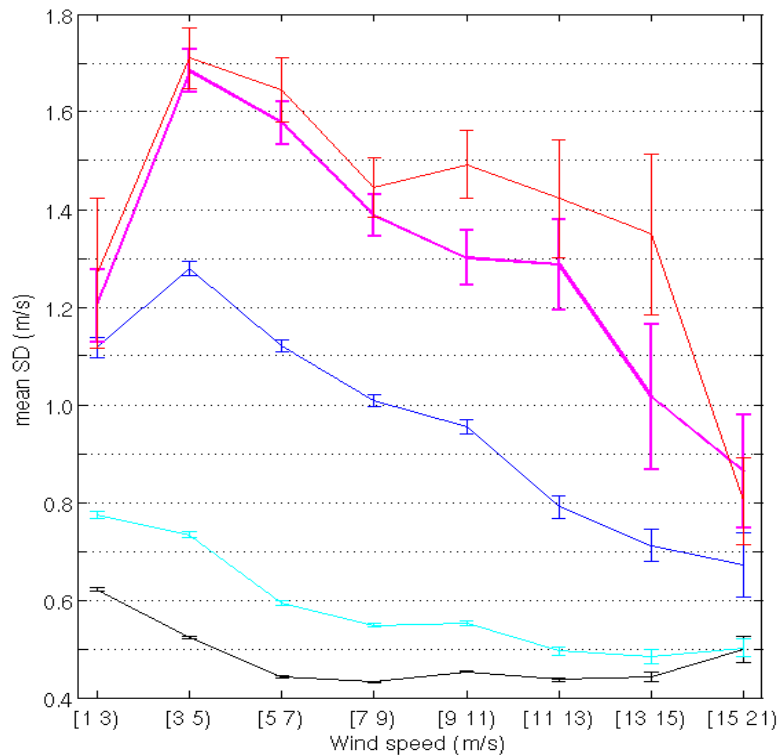


# Wind variability under rainy condntions



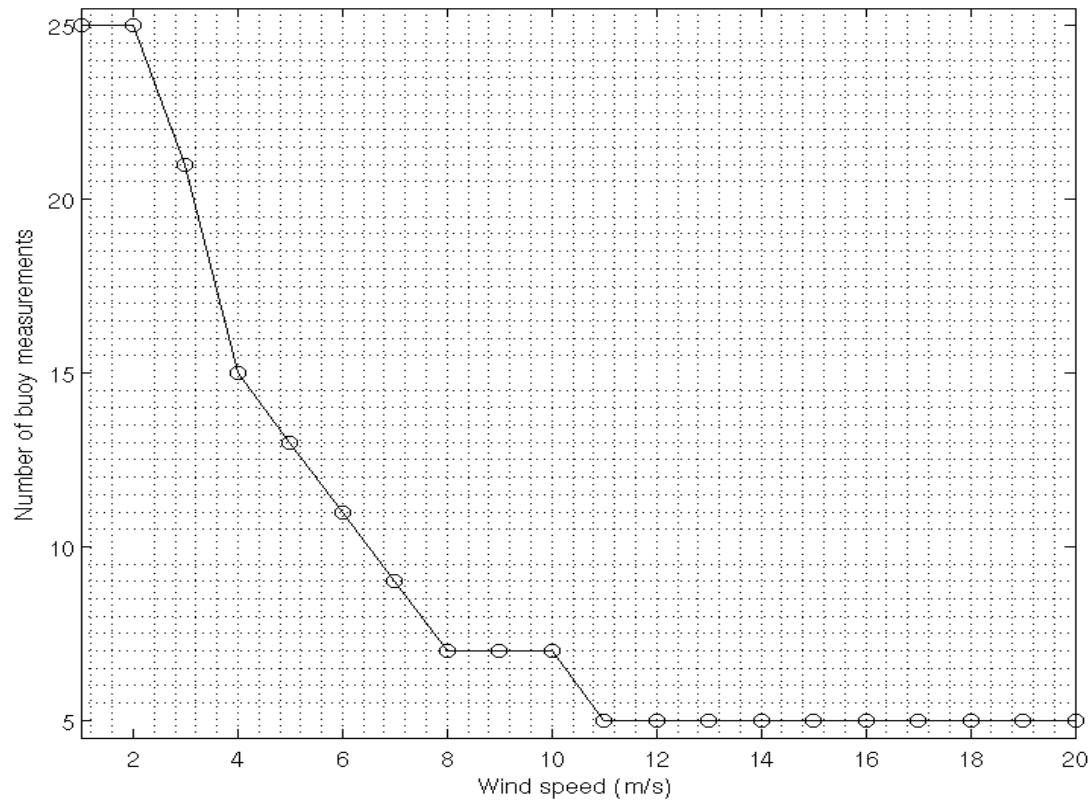
The SD value of (*left-panel*) wind speed and (*right-panel*) direction in terms of mean wind speed and TMI rain rate. All the 13 buoy measurements within  $\pm 1$  hour are used in the assessment.

# Wind variability under rainy condntions



The SD value of (*left-panel*) wind speed and (*right-panel*) direction in terms of mean wind speed and TMI rain rate. Only **N** buoy measurements are used in the assessment.(N depends on wind speed, see the next figure)

# Wind variability under rainy condntions



The number of buoy measurements used to assess wind variability